Effect of squeeze on electrostatic Trivelpiece-Gould wave damping

Arash Ashourvan and Daniel H. E. Dubin

Citation: Physics of Plasmas (1994-present) **21**, 052109 (2014); doi: 10.1063/1.4878319
View online: http://dx.doi.org/10.1063/1.4878319
View Table of Contents: http://scitation.aip.org/content/aip/journal/pop/21/5?ver=pdfcov
Published by the AIP Publishing

Effect of squeeze on electrostatic Trivelpiece-Gould wave damping

Arash Ashourvan and Daniel H. E. Dubin
Department of Physics, University of California at San Diego, La Jolla, California 92093, USA

(Received 13 March 2014; accepted 4 May 2014; published online 27 May 2014)

We present a theory for increased damping of Trivelpiece-Gouid plasma modes on a nonneutral plasma column, due to application of a Debye shielded cylindrically symmetric squeeze potential φ_1. We present two models of the effect this has on the plasma modes: a 1D model with only axial dependence, and a 2D model that also keeps radial dependence in the squeezed equilibrium and the mode. We study the models using both analytical and numerical methods. For our analytical studies, we assume that $\varphi_1/T \ll 1$, and we treat the Debye shielded squeeze potential as a perturbation in the equilibrium Hamiltonian. Our numerical simulations solve the 1D Vlasov-Poisson system and obtain the frequency and damping rate for a self-consistent plasma mode, making no assumptions as to the size of the squeeze. In both the 1D and 2D models, damping of the mode is caused by Landau resonances at energies E_n for which the particle bounce frequency $\omega_b(E_n)$ and the wave frequency ω satisfy $\omega = n\omega_b(E_n)$. Particles experience a non-sinusoidal wave potential along their bounce orbits due to the squeeze potential. As a result, the squeeze induces bounce harmonics with $n > 1$ in the perturbed distribution. The harmonics allow resonances at energies $E_n \leq T$ that cause substantial damping, even when wave phase velocities are much larger than the thermal velocity. In the regime $\omega/k \gg \sqrt{T/m}$ (k is the wave number) and $T \gg \varphi_1$, the resonance damping rate has a $|\varphi_1|^2$ dependence. This dependence agrees with the simulations and experimental results. © *2014 AIP Publishing LLC*.
[http://dx.doi.org/10.1063/1.4878319]

I. INTRODUCTION

Trivelpiece-Gould (TG) modes are electrostatic normal modes of a cylindrical plasma column. For a cold plasma contained in a perfectly conducting cylinder of radius r_w, with uniform plasma density up to the plasma surface at radius $r_p \leq r_w$, the dispersion relation for the TG modes is[1]

$$\omega \approx \omega_p \frac{k_m}{\sqrt{k_\perp^2 + k_m^2}} \left[1 + \frac{3}{2}\left(\frac{k_m v_T}{\omega}\right)^2\right]. \tag{1}$$

The above equation employs the following notation: mode frequency ω, plasma frequency $\omega_p = \sqrt{4\pi q^2 n_0/m_q}$, density n_0, particle charge q, particle mass m_q, thermal velocity $v_T = \sqrt{T/m_q}$, perpendicular wave number $k_\perp$, and axial wave number $k_m = \pi m/L$ (L is the length of the plasma). Throughout the paper, we assume that $L \gg r_w$. For such a thin and long plasma and for cylindrically symmetric modes to the lowest order in r_w/L, the radial wave number is approximated by

$$k_\perp \approx \frac{1}{r_p}\sqrt{\frac{2}{\log(r_w/r_p)}},$$

for the lowest order radial mode, and for modes with one or more radial nodes, $k_\perp r_p \simeq j_{1n}$ where j_{1n} is the nth zero of the Bessel function $J_1(x)$. (However, if $r_p = r_w$, $k_\perp r_p = j_{0n}$.[1])

This paper considers the effect on cylindrically symmetric Trivelpiece-Gould modes of applying a cylindrically symmetric, axially localized "squeeze" potential $\varphi_{sq}(r,z)$ to the plasma column. In experiments, a controlled squeeze potential is created by applying a voltage to a conducting ring encircling the plasma column. Uncontrolled axial squeezes, both magnetic and electrostatic, are ubiquitous in many different experiments, and our work is an attempt to quantify their effect on plasma modes.

We focus on plasma conditions such that the mode phase velocities are much greater than the thermal velocity of the plasma. In such conditions, Landau damping in the absence of squeeze is expected to be negligibly small. The presence of the squeeze potential modifies the orbits of the particles as well as the spatial form of the mode potential, which results in additional resonances at particle bounce frequencies satisfying $\omega_b(E_n) = \omega/n$, where $\omega_b(E)$ is the frequency of axial bounce motion of particles with energy E. Physically, particles moving in z experience a non-sinusoidal mode potential caused by the squeeze, producing high-frequency harmonics that can resonate with the wave frequency to cause Landau damping, even when the mode phase velocity is large compared to the thermal velocity. We will see that these added resonances cause an enhancement to the mode damping rate that has a $|\varphi_1|^2$ dependence. We also derive a real frequency shift proportional to φ_1. These theory results are verified by computer simulations.

Previous work has examined the effect of an axisymmetric squeeze on θ-dependent $\mathbf{E} \times \mathbf{B}$ drift modes, in theory[2,3] and experiment.[4] Enhanced damping due to squeeze was also observed on these modes, but due mainly to collisional effects, caused by a mode-driven discontinuity in the velocity distribution function at the separatrix between passing particles (those with kinetic energy large enough to pass

over the squeeze potential) and particles trapped on either side of the squeeze. While collisional effects can play an important role in TG mode damping, particularly in low temperature multispecies plasmas, we believe that collisions are unimportant in determining the enhanced damping due to squeeze compared to the collisionless effects considered here, in the regime where the collision rate is small compared to the bounce frequency. TG mode frequencies are much higher than those for the $\mathbf{E}\times\mathbf{B}$ drift modes considered previously, and this tends to suppress the separatrix discontinuity that enhances collisional damping.

In Sec. II, we present a 1D model theory for squeezed Trivelpiece-Gould modes, which includes a self-consistent treatment of the mode potential in the presence of a 1D squeeze potential. In the analytical solution of this model, we assume that $\varphi_1/T \ll 1$ and treat its effect with perturbation theory. This naturally neglects trapped particle effects on the modes. We evaluate the mode damping rate and frequency shift from our theory and compare these results to computer simulations, which make no assumptions about the size of φ_1/T, finding good agreement when φ_1/T is small.

In Sec. IV, we extend our method to a cylindrically symmetric r and z dependent plasma of length L trapped in a Malmberg-Penning trap of the same length and wall radius r_w, assuming flat plasma ends that specularly reflect particles. A squeeze potential φ_{sq} is applied to a conducting cylindrical section of width Δ at the axial center of trap. Similar to the 1D model, since the squeeze potential is Debye shielded from the inner plasma, we assume that the Debye shielded squeeze potential energy inside the plasma is small compared to plasma temperature, i.e., $\varphi_1(r,z) \ll T$ and thus neglect trapped particle effects. Using perturbation theory, corrections due to squeeze potential to the r and z dependent eigenmodes and their related eigenfrequencies and damping rates are obtained.

II. 1D MODEL

In this section, we neglect radial variation for simplicity and we assume that the plasma ends are flat, and that particles undergo specular reflection at the ends, $z=\pm L/2$. We also assume that the squeeze potential is symmetric in z with respect to the center of plasma. This is not necessarily the case in the experiments, however, this added symmetry simplifies the problem. In this 1D model, we will find that Eq. (1) still applies, but now $k_\perp$ is an arbitrary parameter. We focus on azimuthally symmetric modes in a strong magnetic field and we assume the following ordering for the time scales:

$$\nu_{col} \ll \omega_b \lesssim \omega \lesssim \omega_p \ll \omega_c. \tag{2}$$

Here, ν_{col} is the collision frequency and $\omega_c = qB/m_q c$ is the cyclotron frequency. Reading from left to right, the first inequality allows us to use collisionless theory to describe the waves; the second inequality is necessary so that waves are not heavily Landau damped; and the fourth assumes a strong magnetic field. In such a strong magnetic field, the distribution of particle guiding centers is described by drift-kinetic equations. Particle motion consists of $\mathbf{E}\times\mathbf{B}$ drift motion across the magnetic field and streaming along the magnetic field in the z direction. Since we assume the plasma consists of one type of particles with charge q, in our calculation, we make use of potential energy instead of electrostatic potential, in order to simplify our notation.

In this 1D strong-magnetic-field model, collisionless plasma dynamics is described by the time evolution of the Vlasov particle density $f(z, v, t)$, a solution of the 1D Vlasov equation

$$\frac{\partial f}{\partial t} + v\frac{\partial f}{\partial z} - \frac{1}{m_q}\frac{\partial \varphi}{\partial z}\frac{\partial f}{\partial v} = 0, \tag{3}$$

where $\varphi(z,t)$ is the potential energy of a particle. This potential energy is the sum of a given time-independent applied external squeeze potential $\varphi_{sq}(z)$, and the plasma response $\varphi_p(z,t)$,

$$\varphi(z,t) = \varphi_{sq}(z) + \varphi_p(z,t), \tag{4}$$

where the plasma response satisfies Poisson's equation

$$\frac{\partial^2 \varphi_p}{\partial z^2} - k_\perp^2 \varphi_p = -4\pi q^2\left(\int dv f - n_0\right). \tag{5}$$

Here, n_0 is the density of a uniform neutralizing background charge (provided by rotation at a given frequency through the uniform magnetic field in the actual plasma system.) We also assume here that "radial dependence" of the plasma potential in our 1D slab model is given by the $k_\perp^2\varphi$ term. In the actual plasma experiments, this term is replaced by the radial part of the Laplacian operator—see Sec. IV for the model including radial dependence.

For our analysis of linear modes, we linearize Eqs. (3) and (4) in the wave potential, writing

$$\varphi_p(z,t) = \varphi_{pe}(z) + \delta\varphi(z,t), \tag{6}$$

and

$$f(z,v,t) = n_0(\mathrm{F}_0(z,v) + \delta \mathrm{f}(z,v,t)). \tag{7}$$

Here, φ_{pe} is the equilibrium plasma potential, $n_0\mathrm{F}_0(z,v)$ is the equilibrium distribution function, and $\delta\varphi$ and δf are the perturbed potential and distribution function, respectively, due to the TG mode. The equilibrium quantities satisfy the time-independent Vlasov-Poisson system

$$v\frac{\partial \mathrm{F}_0}{\partial z} - \frac{1}{m_q}\frac{\partial \varphi_1}{\partial z}\frac{\partial \mathrm{F}_0}{\partial v} = 0, \tag{8}$$

$$\frac{\partial^2 \varphi_{pe}}{\partial z^2} - k_\perp^2 \varphi_{pe} = -4\pi q^2 n_0\left(\int dv \mathrm{F}_0 - 1\right), \tag{9}$$

where

$$\varphi_1(z) = \varphi_{sq}(z) + \varphi_{pe}(z) + C \tag{10}$$

is the total equilibrium potential energy, and C is any constant (we may choose to measure potential energy with respect to any convenient zero value). For our purposes, we

find it convenient to take $C = -\varphi_{sq}(L/2) - \varphi_{pe}(L/2)$, so that (for a symmetric squeeze potential) $\varphi_1(\pm L/2) = 0$. In Sec. II A, we discuss the solution of this coupled equilibrium system for a given symmetric squeeze potential $\varphi_{sq}(z)$.

To determine the dispersion relation for TG waves in the presence of a squeeze potential, we substitute Eqs. (6) and (7) into Eqs. (3) and (5) and linearize in the wave amplitude obtaining the linearized Vlasov-Poisson system

$$\frac{\partial \delta \mathrm{f}}{\partial t} + v\frac{\partial \delta \mathrm{f}}{\partial z} - \frac{1}{m_q}\frac{\partial \varphi_1}{\partial z}\frac{\partial \delta \mathrm{f}}{\partial v} - \frac{1}{m_q}\frac{\partial \delta\varphi}{\partial z}\frac{\partial \mathrm{F}_0}{\partial v} = 0, \tag{11}$$

$$\frac{\partial^2 \delta\varphi}{\partial z^2} - k_\perp^2 \delta\varphi = -4\pi q^2 n_0 \int dv \delta \mathrm{f}. \tag{12}$$

We consider solutions of these coupled linearized equations in Sec. II B.

A. Squeezed thermal equilibrium

The plasma in this model is a slab of width L running from $-L/2 \le z \le L/2$. In the absence of a squeeze, it has uniform density n_0. We assume that the applied squeeze potential $\varphi_{sq}(z)$ is symmetric with respect to the center of plasma. It has a maximum $\varphi_{sq}^{\max} = \varphi_{sq}(0)$ and minima at the plasma ends. Then the solution of Eq. (8) for the equilibrium distribution function is $\mathrm{F}_0 = \mathrm{F}_0(H_0(z,v))$, where H_0 (z,v) is the Hamiltonian of the plasma equilibrium given by

$$H_0 = m_q v^2/2 + \varphi_1(z). \tag{13}$$

For any given function form of F_0 (H_0), Eqs. (8)–(10), and (13) can be solved for the plasma potential energy $\varphi_{pe}(z)$, for given boundary conditions on Eq. (9). We assume periodic boundary conditions with period L. The functional form we choose for F_0 (H_0) is the Boltzmann distribution

$$\mathrm{F}_0(H_0(z,v)) = \frac{e^{-\frac{H_0}{T}}}{\sqrt{2\pi T/m_q}\int_{-L/2}^{L/2} e^{-\frac{\varphi_1(z)}{T}} d(z/L)}, \tag{14}$$

normalized so that

$$\int_{-\infty}^{\infty}\int_{-L/2}^{L/2} \mathrm{F}_0 dv dz = L. \tag{15}$$

We are particularly interested in a case where the squeeze potential is Debye shielded to the extent that the equilibrium potential energy φ_1 inside the plasma is much smaller than the average kinetic energy; i.e., $\varphi_1/T \ll 1$. In this situation, we can expand Eq. (9) to the first order in φ_1/T and get the following relation:

$$(-k_\perp^2 + \partial_z^2)\varphi_{pe} = \lambda_D^{-2}(\varphi_1 - \langle\varphi_1\rangle), \tag{16}$$

where $\lambda_D = \sqrt{T/4\pi q^2 n_0}$ is the Debye length, and $\langle\cdot\rangle = \int_{-L/2}^{L/2} dz/L$. For a squeeze potential, which is symmetric with respect to the center of the plasma, we have the following representations (using the periodic boundary conditions):

$$\varphi_1(z) = \langle\varphi_1\rangle + \sum_{n=1}^{\infty} \varphi_n^1 \cos\left[\frac{2n\pi}{L}\left(z + \frac{L}{2}\right)\right], \tag{17}$$

$$\varphi_{sq}(z) = \langle\varphi_{sq}\rangle + \sum_{n=1}^{\infty} \varphi_{sq}^n \cos\left[\frac{2n\pi}{L}\left(z + \frac{L}{2}\right)\right]. \tag{18}$$

From Eqs. (16), (17), and (10), we can solve for φ_1, the Debye shielded squeeze potential

$$\begin{aligned}\langle\varphi_1\rangle &= \langle\varphi_{sq}\rangle - \varphi_{pe}(L/2) - \varphi_{sq}(L/2),\\ \varphi_n^1 &= \frac{(k_\perp^2 + k_{2n}^2)\lambda_D^2 \varphi_{sq}^n}{(k_\perp^2 + k_{2n}^2)\lambda_D^2 + 1},\end{aligned} \tag{19}$$

$$\varphi_{pe}(L/2) = -\sum_{n=1}^{\infty} \frac{\varphi_{sq}^n}{(k_\perp^2 + k_{2n}^2)\lambda_D^2 + 1}, \tag{20}$$

where $k_n = n\pi/L$.

As a model for numerical work, the applied squeeze potential $\varphi_{sq}(z)$ is taken as a Gaussian function with maximum $\varphi_{sq}^{\max}$ at the center of plasma $z = 0$ and width Δ

$$\varphi_{sq}(z) = \varphi_{sq}^{\max} e^{-\frac{z^2}{2\Delta^2}}. \tag{21}$$

From Eq. (19), we can see that the magnitude of the potential inside the plasma is linearly proportional to the magnitude of the squeeze potential in the regime where $\varphi_1 \ll T$. For future reference, we define the maximum of the Debye shielded squeeze potential at $z = 0$ as $\varphi_s \equiv \varphi_1(0)$.

B. Obtaining the matrix linear dispersion relation

In this section, we solve the linearized Vlasov equation (11), for the perturbed distribution function $\delta \mathrm{f}(z,v)$, and use the linearized Poisson's equation (12) to obtain a dispersion relation for the electrostatic potential energy $\delta\varphi$ in the plasma waves. We define the scaled potential $\bar{\varphi}_1$ and scaled energy variable u as

$$\bar{\varphi}_1(z) = \varphi_1(z)/T, \tag{22}$$

$$u = m_q v^2/2T + \varepsilon\bar{\varphi}_1(z). \tag{23}$$

Here, ε is an auxiliary smallness parameter, pertinent for a system where the squeeze is small, $\varphi_1/T \ll 1$. At the end of the calculation, ε will be set to 1. We rewrite the equilibrium distribution function in terms of u as

$$\mathrm{F}_0(u) = \frac{e^{-u}}{\sqrt{2\pi T/m_q}\int_{-L/2}^{L/2} e^{-\varepsilon\bar{\varphi}_1(z)} d(z/L)}. \tag{24}$$

To solve for $\delta \mathrm{f}$, we note that particles perform a periodic bounce motion along their orbits in the equilibrium potential $\varphi_1(z)$. Thus, in order to simplify our calculations, we use the canonical action-angle variables of the orbits, ψ and I, which are defined by

$$\psi = \omega_b \int_{z_0}^{z} \frac{dz}{v(z)}, \qquad I = \frac{1}{2\pi}\oint p_z dz. \tag{25}$$

Here, the velocity of a particle with scaled energy u is given by

$$v(z) = v_T\sqrt{2(u - \varepsilon\bar{\varphi}_1(z))}. \tag{26}$$

The bounce frequency ω_b is the fundamental frequency of the periodic orbits and can be calculated from

$$\omega_b = 2\pi/\tau, \quad \tau = \oint \frac{dz}{v(z)}, \tag{27}$$

where τ is the time period of one cycle of motion for particle of action I. For particles with energy $u > \varepsilon\bar{\varphi}_s$ (where $\bar{\varphi}_s = \bar{\varphi}_1(0)$), which we term "passing particles," this cycle of motion is from $-L/2$ to $L/2$ and back. For particles with energy $u < \varepsilon\bar{\varphi}_s$, which are trapped on one side of the squeeze, there is a turning point as particles reflect from the squeeze potential. The bounce frequency of the cycle of motion ω_b can also be expressed as

$$\omega_b(I) = T\partial u/\partial I. \tag{28}$$

Using Eq. (25), ψ can be written as a function of z and scaled energy u

$$\begin{aligned}\psi &= \frac{2\pi}{\oint \frac{dz}{\sqrt{(2(u-\varepsilon\bar{\varphi}_1(z))}}} \int_{z_0}^{z} \frac{dz}{v_T\sqrt{2(u-\varepsilon\bar{\varphi}_1(z))}},\\ &= \frac{2\pi}{\oint \frac{dz}{\sqrt{1-\varepsilon\bar{\varphi}_1(z)/u}}} \int_{z_0}^{z} \frac{dz}{\sqrt{1-\varepsilon\bar{\varphi}_1(z)/u}},\\ &= \psi(z, \varepsilon/u).\end{aligned} \tag{29}$$

As a result of inverting Eq. (29), we have

$$z = z(\psi, \varepsilon/u), \tag{30}$$

where z is a periodic function of ψ. The mode potential $\delta\varphi(z)$ can then be written in terms of action-angle variables. First, we note that for a long thin plasma where $\omega \ll \omega_p$, to the zeroth order in ω/ω_p the boundary condition on the mode potential at the plasma ends is approximately $\partial_z\delta\varphi(\pm L/2) \approx 0$.[5] Therefore, the standing mode potential can be written as

$$\delta\varphi(z,t) = \sum_{m=1}^{\infty}\left(e^{-i\omega t}\delta\phi_m + e^{i\omega t}\delta\phi_m^*\right)\cos[k_m(z+L/2)], \tag{31}$$

where $k_m = m\pi/L$, $\delta\phi_m = \delta\phi_m^r + i\delta\phi_m^i$ is the mth complex Fourier component in the position space and $\omega = \omega_r + i\gamma$ is the complex mode frequency. Alternatively, we can write the above equation in terms of strictly real functions as

$$\begin{aligned}\delta\varphi(z,t) = 2\sum_{m=1}^{\infty} e^{-\gamma t}\left(\delta\phi_m^i \sin(\omega_r t) + \delta\phi_m^r \cos(\omega_r t)\right)\\ \times \cos[k_m(z+L/2)].\end{aligned} \tag{32}$$

Next, since z is periodic in ψ, we can write the z-dependence as a Fourier series in ψ

$$\cos\left[k_m\left(z(\psi,\varepsilon/u) + \frac{L}{2}\right)\right] = \sum_{n=-\infty}^{\infty} C_m^n(\varepsilon/u)e^{in\psi}, \tag{33}$$

where the connection coefficients C_m^n are

$$C_m^n(\varepsilon/u) = \frac{1}{2\pi}\int_0^{2\pi} e^{-in\psi}\cos\left[k_m\left(z(\psi,\varepsilon/u) + \frac{L}{2}\right)\right] d\psi. \tag{34}$$

These coefficients connect Fourier representations in z and ψ. Using these coefficients, we can write

$$\begin{aligned}\delta\varphi(\psi,\varepsilon/u;t) = \sum_{n=-\infty}^{\infty}\sum_{m=1}^{\infty}(\delta\phi_m C_m^n(\varepsilon/u)e^{i(n\psi-\omega t)}\\ + \delta\phi_m^* C_m^{-n}(\varepsilon/u)e^{-i(n\psi-\omega t)}).\end{aligned} \tag{35}$$

Since u (or action I) is a constant of the unperturbed motion and $\psi = \omega_b t + \psi(0)$, relation (35) expresses the mode potential as experienced by a particle with scaled energy u, as a function of time along its unperturbed orbit.

The form of the mode potentials as a function of z and the mode eigenfrequencies can be obtained by simultaneously solving the linear 1D Vlasov equation (11) and the Poisson equation (12), where the mode perturbation to the distribution function is of the form

$$\delta f(z,v;t) = \delta f(z,v)e^{-i\omega t} + c.c. \tag{36}$$

Substituting for $\delta\varphi$ from Eq. (31), multiplying both sides of Eq. (12) by $\frac{2}{L}e^{-i\omega t}\cos[k_m(z+L/2)]$, integrating in time over a period $(2\pi/\omega)$, and in z over the whole length of the plasma, from $-L/2$ to $L/2$ we have the following series of equations:

$$\begin{aligned}(k_\perp^2 + k_m^2)\delta\phi_m = 4\pi q^2 n_0 \frac{2}{L}\int_{-L/2}^{L/2}\int_{-\infty}^{\infty}\delta f(z,v)\\ \times \cos\left[k_m\left(z+\frac{L}{2}\right)\right]dzdv,\end{aligned} \tag{37}$$

where $m = 1, 2, \ldots$. The linear Vlasov equation (11) can also be written in terms of canonical action-angle variables

$$\partial_t\delta f + \omega_b\partial_\psi\delta f - \partial_\psi\delta\varphi\partial_I F_0(I) = 0. \tag{38}$$

This can be solved by expressing δf in terms of action-angle variables

$$\delta f(\psi, I; t) = \sum_{n=-\infty}^{\infty}\delta f_n(I)e^{i(n\psi-\omega t)} + c.c. \tag{39}$$

Substituting from Eqs. (35) and (39) in Eq. (38) and solving for $\delta f_n(I)$, we obtain

$$\delta f_n(I) = \frac{n\omega_b \sum_{\bar{m}=1}^{\infty} \delta\phi_{\bar{m}} C_{\bar{m}}^n(\varepsilon/u) \mathrm{F}_0(I)/T}{\omega - n\omega_b}. \tag{40}$$

On the right hand side of Eq. (40), we used

$$\frac{\partial}{\partial I}\mathrm{F}_0(u) = T^{-1}\left(\frac{du}{dI}\right)\frac{\partial}{\partial u}\mathrm{F}_0(u) = -\omega_b \frac{\mathrm{F}_0}{T},$$

where F_0 is given in Eq. (24). Since ψ and I are canonical coordinates, $dzdp_z = d\psi dI$ and we can exchange the integration over (z, v) variables (on the right hand side of Eq. (37)) to (ψ, I) variables. Performing the integral in Eq. (37) over ψ from 0 to 2π using Eqs. (34) and (40), we obtain

$$\delta\phi_m - \frac{\omega_p^2}{K_m^2}\frac{4\pi}{LT}\sum_{n=-\infty}^{\infty}\int_{\mho} dI \frac{n\omega_b \mathrm{F}_0(I)}{\omega - n\omega_b}\sum_{\bar{m}=1}^{\infty}\delta\phi_{\bar{m}} C_{\bar{m}}^n(\varepsilon/u) \times C_m^{-n}(\varepsilon/u) = 0, \tag{41}$$

where $K_n = \sqrt{k_\perp^2 + k_n^2}$ is the total wave number, and $\mho$ denotes integration with respect to I, performed in the complex plane below the pole (using the Landau contour[6]). Due to the symmetry of the squeeze, we have $C_m^n(\varepsilon/u) = C_m^{-n}(\varepsilon/u)$. Furthermore, in Eq. (41), we will neglect trapped particles, assuming $\bar{\varphi}_s \ll 1$, and we will only integrate over the energies of the passing particles, i.e., $u > \varepsilon\bar{\varphi}_s$. Thus, Eq. (41) becomes

$$\delta\phi_m - \frac{\omega_p^2}{K_m^2}\frac{8}{\sqrt{2\pi}v_T^2\langle e^{-\varepsilon\bar{\varphi}_1}\rangle}\sum_{n=1}^{\infty}\int_{\varepsilon\bar{\varphi}_s}^{\infty} du \frac{\bar{\omega}_b(u,\varepsilon)e^{-u}}{(\bar{\omega}/n)^2 - \bar{\omega}_b(u,\varepsilon)^2} \times \sum_{\bar{m}=1}^{\infty}\delta\phi_{\bar{m}} C_{\bar{m}}^n(\varepsilon/u) C_m^n(\varepsilon/u) = 0, \tag{42}$$

where we used $\omega_b = Tdu/dI$ and Eq. (24). Also we define the scaled bounce frequency $\bar{\omega}_b(u,\varepsilon)$ as $\bar{\omega}_b(u,\varepsilon) = \omega_b/k_1 v_T$, and the (complex) scaled mode frequency $\bar{\omega} = \omega/k_1 v_T$. Equation (42) is a linear, complex, matrix eigenvalue equation which can be written in the simple matrix form as

$$\mathbf{M}(\bar{\omega},\varepsilon).\mathbf{e} = 0, \tag{43}$$

where the dispersion matrix $\mathbf{M}$ and eigenvector $\mathbf{e}$ are given by

$$M^{m\bar{m}}(\bar{\omega},\varepsilon) = \delta_{m\bar{m}} - \frac{8(K_m\lambda_D)^{-2}}{\sqrt{2\pi}\langle e^{-\varepsilon\bar{\varphi}_1}\rangle}\sum_{n=1}^{\infty}\int_{\varepsilon\bar{\varphi}_s}^{\infty} du \times \frac{\bar{\omega}_b(u,\varepsilon)e^{-u}}{(\bar{\omega}/n)^2 - \bar{\omega}_b(u,\varepsilon)^2} C_{\bar{m}}^n(\varepsilon/u) C_m^n(\varepsilon/u), \tag{44}$$

$$\mathbf{e}^T = (\delta\phi_1, \delta\phi_2, \ldots). \tag{45}$$

Equation (43) is solved by finding complex frequencies $\bar{\omega}$ such that an eigenvalue of $\mathbf{M}$ equals zero. The corresponding eigenvector in the nullspace of $\mathbf{M}$ provides the Fourier components of $\delta\varphi(z)$. Different Fourier components of the mode (elements of the right hand side of Eq. (45)) are coupled through the off-diagonal elements of $\mathbf{M}$, which are generated by the squeeze potential.

C. Perturbation method for the small φ_1/T regime

In order to obtain the eigenvalues, eigenvectors, and the damping rate of the modes, we will use a perturbation approach and expand the dispersion relation in orders of ε as the smallness parameter. We Taylor expand the dispersion matrix $\mathbf{M}$ for small ε in Eq. (44)

$$\mathbf{M}(\bar{\omega},\varepsilon) = \mathbf{M}(\bar{\omega},0) + \partial_\varepsilon\mathbf{M}(\bar{\omega},0)\varepsilon + \frac{1}{2}\partial_\varepsilon^2\mathbf{M}(\bar{\omega},0)\varepsilon^2 + \ldots. \tag{46}$$

We have the following series expansions in terms of ε:

$$\mathbf{M} = \mathbf{M}_0 + \mathbf{M}_1\varepsilon + \mathbf{M}_2\varepsilon^2 + \ldots, \tag{47}$$

$$\mathbf{e} = \mathbf{e}_0 + \mathbf{e}_1\varepsilon + \mathbf{e}_2\varepsilon^2 + \ldots, \tag{48}$$

$$\bar{\omega} = \bar{\omega}_0 + \bar{\omega}_1\varepsilon + \bar{\omega}_2\varepsilon^2 + \ldots, \tag{49}$$

where

$$\mathbf{M}_0 = \mathbf{M}(\bar{\omega},0),\ \ \mathbf{M}_1 = \partial_\varepsilon\mathbf{M}(\bar{\omega},0),\ \ \mathbf{M}_2 = \frac{1}{2}\partial_\varepsilon^2\mathbf{M}(\bar{\omega},0). \tag{50}$$

Details of the calculation of $\mathbf{M}_0$, $\mathbf{M}_1$, and $\mathbf{M}_2$ are given in Appendix B. The complex column vectors $\mathbf{e}_0$, $\mathbf{e}_1$, $\mathbf{e}_2$ and complex frequencies $\bar{\omega}_0, \bar{\omega}_1, \bar{\omega}_2$ determine the spatial form and complex frequency of the eigenfunctions in the presence of a small squeeze potential.

Using relations (47) through (49), we rewrite the dispersion relation (43), collect the terms of orders ε^0, ε^1 and ε^2 and set the dispersion relation at each order to zero separately.

1. Zeroth order in ε

The zeroth order dispersion relation (for an unsqueezed plasma) is given by

$$\mathbf{M}_0(\bar{\omega}_0^m).\mathbf{e}_0^m = 0, \tag{51}$$

where $\bar{\omega}_0^m$ is the zeroth order, complex eigenfrequency of mode m. From Eq. (B9), the matrix $\mathbf{M}_0$ is, in component form

$$M_0^{\bar{m}m}(\bar{\omega}) = \left(1 + \frac{1}{\lambda_D^2 K_m^2}\mathrm{W}(\bar{\omega}/m)\right)\delta_{\bar{m}m}. \tag{52}$$

Thus, we obtain the following zeroth order dispersion relation for mode m:

$$1 + \frac{1}{\lambda_D^2 K_m^2}\mathrm{W}\left(\bar{\omega}_0^m/m\right) = 0, \tag{53}$$

where the function $\mathrm{W}(b)$ is defined as

$$\mathrm{W}(b) = \frac{1}{\sqrt{2\pi}}\int_{\mho}\frac{xe^{-x^2/2}dx}{x-b}. \tag{54}$$

Equation (51) is the TG mode dispersion relation of an unsqueezed plasma. Since $\mathbf{M}_0$ is a diagonal matrix, each Fourier cosine function in Eq. (31) is an eigenmode. Thus, the zeroth order eigenvector for the mode is

$$\left(\mathbf{e}_0^m\right)_l = \delta_{l,m}\delta\phi_m^m. \tag{55}$$

The zeroth order eigenfrequency $\bar{\omega}_0^m$ is obtained by solving Eq. (53). For weakly damped modes with frequency $\bar{\omega}_0^m = \bar{\omega}_{0r}^m + i\bar{\gamma}_0^m$, the scaled frequency and the damping rate are given by

$$1 + \frac{1}{\lambda_D^2 K_m^2}\mathrm{Re}\,\mathrm{W}\left(\bar{\omega}_{0r}^m/m\right) = 0, \tag{56}$$

$$\bar{\gamma}_0^m = -\frac{\pi\bar{\omega}_{0r}^m e^{-\frac{(\bar{\omega}_{0r}^m)^2}{2m^2}}}{\mathrm{P}\int_{-\infty}^{\infty}\frac{ve^{-v^2/2}dv}{\left(\bar{\omega}_{0r}^m/m - v\right)^2}}. \tag{57}$$

Since we are dealing with linear modes, the mode amplitude $\delta\phi_m^m$ in Eq. (56) is an arbitrary parameter, which we take to be real. In Eq. (57), $\bar{\gamma}_0^m$ is obtained by perturbation, with the assumption that $\bar{\omega}_{0r}^m \gg \bar{\gamma}_0^m$. When $\bar{\omega}_{0r}^m/m \gg 1$, the Landau-damping damping rate $\bar{\gamma}_0^m$ for the unsqueezed plasma is exponentially small.

Both real and imaginary parts of the zeroth-order (unsqueezed) scaled phase velocity $\bar{\omega}_0/m$ are functions only of a single parameter, $K_m\lambda_D$. In the limit that the plasma is cold, so that $K_m\lambda_D \ll 1$, the solution of Eq. (56) is

$$\frac{\bar{\omega}_{0r}^2}{m^2} = \frac{1}{\left(K_m\lambda_D\right)^2} + 3 + 6\left(K_m\lambda_D\right)^2 + 24\left(K_m\lambda_D\right)^4 + 180\left(K_m\lambda_D\right)^6 + \ldots. \tag{58}$$

The first two terms in this asymptotic series are equivalent to Eq. (1).

2. First order in ε

We obtain the first order correction to the mode frequency $\bar{\omega}_1^m = \bar{\omega}_{1r}^m + i\bar{\gamma}_1^m$, and the first order correction to the eigenvector $\mathbf{e}_1^m$ from the first order dispersion relation given by

$$\mathbf{M}_0(\bar{\omega}_0^m).\mathbf{e}_1^m + \bar{\omega}_1^m\partial_{\bar{\omega}}\mathbf{M}_0(\bar{\omega}_0^m).\mathbf{e}_0^m + \mathbf{M}_1(\bar{\omega}_0^m).\mathbf{e}_0^m = 0, \tag{59}$$

where from Eq. (B16) the components of the matrix $\mathbf{M}_1$ are given by the expression

$$M_1^{mn} = -\frac{4}{K_m^2\lambda_D^2}\left(\frac{m^2}{\bar{\omega}^2}[1 - \mathrm{W}(\bar{\omega}/m)]\alpha_n^m + \frac{n^2}{\bar{\omega}^2}[1 - \mathrm{W}(\bar{\omega}/n)]\alpha_m^n\right), \tag{60}$$

where the coefficients α_m^n are first-order in ε corrections to the Fourier connection coefficients C_m^n, given by

$$\alpha_m^n = \begin{cases} \frac{m}{8}\left(\frac{\bar{\varphi}^1_{|m-n|/2}}{m-n} + \frac{\bar{\varphi}^1_{|m-n|/2}}{m+n}\right), & m \neq \pm n \\ \frac{\bar{\varphi}_m^1}{16}, & m = \pm n. \end{cases} \tag{61}$$

From Eq. (59), we solve for the first order correction to $\mathbf{e}^m$, which is given by the components

$$\left(\mathbf{e}_1^m\right)_j = -\frac{M_1^{jm}(\bar{\omega}_0^m)}{M_0^{jj}(\bar{\omega}_0^m)}\delta\phi_m^m, \quad j \neq m \tag{62}$$

and $\left(\mathbf{e}_1^m\right)_m = 0$. Using relation (32), we can write the squeezed eigenmode m up to the first order in ε as

$$\begin{aligned}\delta\varphi^m(z,t) = {} & 2\delta\phi_m^m e^{-\gamma t}\cos(\omega_r t)\cos[k_m(z+L/2)] \\ & + 2\varepsilon\sum_{j\neq m}^{\infty}\mathrm{Im}[\delta\phi_j^m]\cos[k_j(z+L/2)]e^{-\gamma t}\sin(\omega_r t) \\ & + 2\varepsilon\sum_{j\neq m}^{\infty}\mathrm{Re}[\delta\phi_j^m]\cos[k_j(z+L/2)]e^{-\gamma t}\cos(\omega_r t),\end{aligned} \tag{63}$$

where $\delta\varphi_j^m = \left(\mathbf{e}_1^m\right)_j$ (see Eqs. (45) and (62)). Contributions to the mode potential from wave numbers, $k_j \neq k_m$ are linearly proportional to the squeeze amplitude φ_s. These terms $(j \neq m)$ are also linearly proportional to the amplitude of the unsqueezed mode potential $\delta\phi_m^m$ (as seen from Eq. (62)). There are $\sin(\omega_r t)$ dependent as well as $\cos(\omega_r t)$ dependent contributions from the $j \neq m$ terms to the mode potential. Using Eq. (62), the spatial dependence of $j \neq m$ terms with $\sin(\omega_r t)$ and $\cos(\omega_r t)$ time dependence are

$$\delta\phi_{\sin}^m(z) = -2\varepsilon\delta\phi_m^m\sum_{j\neq m}^{\infty}\mathrm{Im}\left[\frac{M_1^{jm}(\bar{\omega}_0^m)}{M_0^{jj}(\bar{\omega}_0^m)}\right]\cos[k_j(z+L/2)], \tag{64}$$

$$\delta\phi_{\cos}^m(z) = -2\varepsilon\delta\phi_m^m\sum_{j\neq m}^{\infty}\mathrm{Re}\left[\frac{M_1^{jm}(\bar{\omega}_0^m)}{M_0^{jj}(\bar{\omega}_0^m)}\right]\cos[k_j(z+L/2)]. \tag{65}$$

Figure 1 depicts $\delta\phi_{\sin}^m/(\bar{\varphi}_s\delta\phi_m^m)$ and $\delta\phi_{\cos}^m/(\bar{\varphi}_s\delta\phi_m^m)$, for mode $m = 1$, with $k_\perp L = 15\pi$ and plasma frequencies $\omega_p/k_1 v_T = 90$ and $\omega_p/k_1 v_T = 200$. We divide out the scaled squeeze potential maximum value $\bar{\varphi}_s$ so that the resulting functions are independent of the size of the squeeze. The $\sin(\omega_r t)$ dependent part of the mode potential becomes smaller for larger values of the phase velocity.

The shift in the frequency of the mode due to the squeeze is found by taking the product of Eq. (59) from left with $(\mathbf{e}_0^m)^T$. The first term will result in zero, since $(\mathbf{e}_0^m)^T.\mathbf{M}_0(\omega_0^m) = 0$. Solving for $\bar{\omega}_1^m$, we obtain

$$\bar{\omega}_1^m = -\frac{M_1^{mm}(\bar{\omega}_0^m)}{\partial_{\bar{\omega}}M_0^{mm}(\bar{\omega}_0^m)}. \tag{66}$$

Substituting from Eq. (60) for the numerator and from Eq. (52) for the denominator, we write the above equation as

$$\bar{\omega}_1^m = \frac{\frac{m^2}{2(\bar{\omega}_0^m)^2}\left[1 - \mathrm{W}(\bar{\omega}_0^m/m)\right]\bar{\varphi}_m^1}{\partial_{\bar{\omega}}\mathrm{W}(\bar{\omega}_0^m/m)}, \tag{67}$$

where $\bar{\varphi}_m^1 \equiv \varphi_m^1/T$ is the scaled Fourier component of the squeeze potential [see Eq. (17)]. Using the following relation:

$$\partial_b\mathrm{W}(b) \equiv -[1 - \mathrm{W}(b)]/b - b\mathrm{W}(b), \tag{68}$$

and in Eq. (53), we can write Eq. (67) as

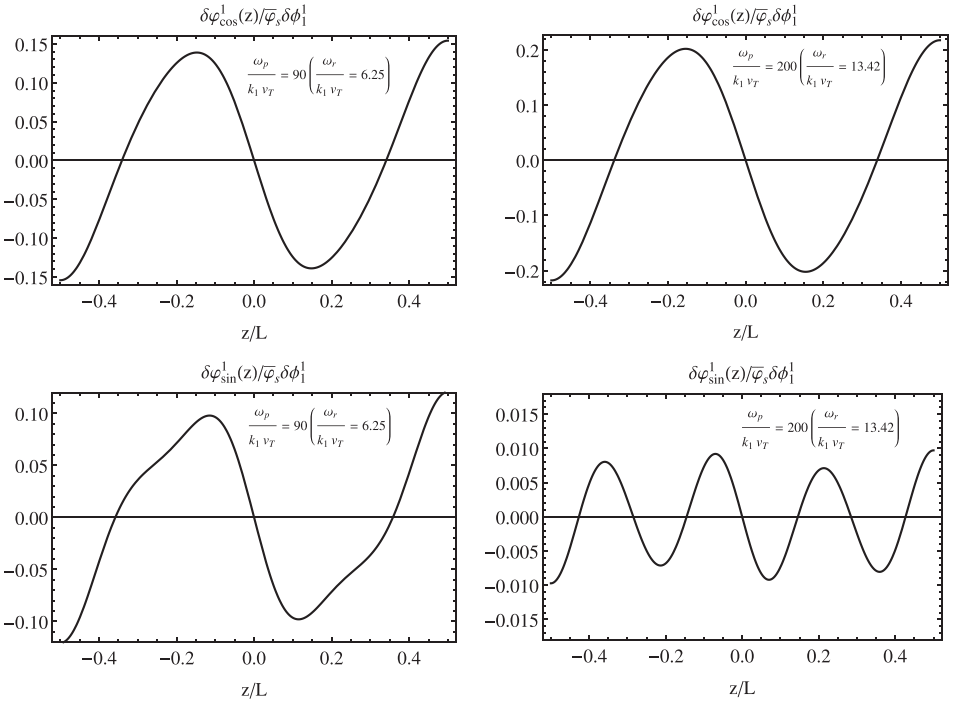

FIG. 1. The change to the spatial dependence of mode potential for mode $m=1$, with $\cos(\omega_r t)$ and $\sin(\omega_r t)$ time dependence, in a plasma with $k_\perp L = 15\pi$ and scaled plasma frequencies $\omega_p/k_1 v_T = 90$ and $\omega_p/k_1 v_T = 200$, corresponding to mode phase velocities $\omega_{r_0}/k_1 v_T = 6.25$ and 13.42, respectively.

$$\bar{\omega}_1^m = \frac{m\bar{\varphi}^1_m/2}{\frac{\lambda_D^2 K_m^2}{1+\lambda_D^2 K_m^2}\left(\frac{\bar{\omega}_0^m}{m}\right)^3 - \frac{\bar{\omega}_0^m}{m}}. \tag{69}$$

Furthermore, with the assumption that $\bar{\omega}^m_{0r} \gg \bar{\gamma}^m_0$, we can write the real and imaginary part of $\bar{\omega}^m_1 = \bar{\omega}^m_{1r} + i\bar{\gamma}^m_1$ as

$$\bar{\omega}^m_{1r} = -\frac{1+\lambda_D^2 K_m^2}{1-\lambda_D^2 K_m^2\left[\left(\frac{\bar{\omega}^m_{0r}}{m}\right)^2 - 1\right]}\frac{m^2}{\bar{\omega}^m_{0r}}\frac{\bar{\varphi}^1_m}{2}, \tag{70}$$

$$\bar{\gamma}^m_1 = -\frac{\bar{\gamma}^m_0}{\bar{\omega}^m_{0r}}(1-\lambda_D^2 K_m^2)\frac{1-\lambda_D^2 K_m^2\left[3\left(\frac{\bar{\omega}^m_{0r}}{m}\right)^2 - 1\right]}{\left(1-\lambda_D^2 K_m^2\left[\left(\frac{\bar{\omega}^m_{0r}}{m}\right)^2 - 1\right]\right)^2}\frac{m\bar{\varphi}^1_m}{2}. \tag{71}$$

From Eq. (71), we see that when $\bar{\omega}^m_0 \gg m$, the first order correction to the damping rate is exponentially small

$$\bar{\gamma}^m_1 \propto \bar{\gamma}^m_0 \propto e^{-\frac{(\bar{\omega}^m_0)^2}{2m^2}} \approx 0, \quad \bar{\omega}^m_{0r} \gg m. \tag{72}$$

The real frequency shift given by Eq. (70) can be rewritten as

$$\bar{\omega}^m_{1r} = \bar{\omega}^m_{0r}\bar{\varphi}^1_m g(K_m\lambda_D), \tag{73}$$

where the function $g(x)$ is found by substitution of Eq. (58) into Eq. (70)

$$g(x) = \frac{1}{4} - \frac{7}{8}x^2 - \frac{21}{32}x^4 - \frac{747}{64}x^6 - \ldots, \quad x \ll 1. \tag{74}$$

Equation (73) can be expressed in terms of the externally applied squeeze potential $\varphi_{sq}(z)$ using Eq. (19)

$$\omega^m_{1r} = \omega^m_{0r}\frac{K^2_{2m}}{1+K^2_{2m}\lambda_D^2}\frac{\varphi^m_{sq}}{m_q\omega_p^2}g(K_m\lambda_D). \tag{75}$$

To lowest order in $K_m\lambda_D$, Eq. (75) describes a temperature-independent frequency shift due to the external squeeze potential

$$\omega^m_{1r} = \omega^m_{0r}K^2_{2m}\frac{\varphi^m_{sq}}{4m_q\omega_p^2}, \quad K_m\lambda_D \to 0. \tag{76}$$

Equation (76) shows that in order for the perturbation theory to be valid, the external squeeze potential need not be small compared to T. Rather, the requirement that perturbation theory be valid is $\varphi_{sq} \ll m_q\omega_p^2/K^2_{2m}$. The right-hand side is typically on the order of the plasma space-charge potential energy. This inequality is consistent with $\varphi_1 \ll T$, since Eq. (19) implies that $\varphi^1_m \simeq K^2_{2m}\lambda_D^2\varphi^m_{sq}$ at low temperatures where $K_{2m}\lambda_D \ll 1$.

Figure 2 is the plot of mode frequency vs. the magnitude of the Debye shielded squeeze potential $\varphi_s \equiv \varphi_1(0)$. Frequencies calculated from the perturbation theory are the sum of the zeroth order frequency calculated from Eq. (56), plus the first order correction to mode frequency using the relation (70), which is depicted as a solid line. We use the same form for the squeeze as before (Eq. (21)). Computer simulation results obtained from the 1D Vlasov-Poisson simulations (described in Sec. III) are depicted with circles. The mode frequency is lowered for positive squeeze potential and raised for negative squeeze potential. This is due to the fact that the density perturbation in the mode, which for $m=1$ is sloshing left and right with its maximum velocity at the center of plasma, has to travel up and down the squeeze, which acts as a kinetic barrier (for positive squeeze). This increases the oscillation time period and hence, lowers the mode frequency. On the other hand, for a negative squeeze,

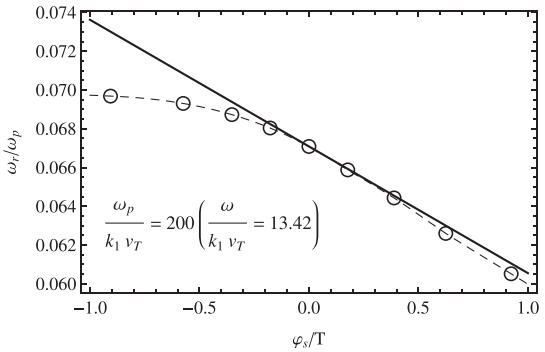

FIG. 2. The real part of the mode frequency ω_r/ω_p vs. the size of the Debye shielded squeeze potential φ_s/T for mode $m=1$, where $\varphi_s \equiv \varphi_1(0)$, for $\omega_p/k_1 v_T = 200$ (which implies $\omega_{0r}/k_1 v_T = 13.42$). Analytically calculated results, shown here with a solid line, are up to the first order in φ_s/T using Eq. (70); computer simulation results are shown with circles.

the oscillation time period decreases since the density perturbation speeds up as it passes the center of plasma, and as a result, mode frequency increases.

3. Fluid theory for the frequency correction

It is also possible to understand the TG mode frequency shift (but not the damping) caused by applied squeeze using fluid theory rather than kinetic theory. In fluid theory, the equilibrium plasma density varies in z due to the squeeze, and this density variation affects the mode frequency. The density variation is given by the Boltzmann factor

$$n_{eq}(z) = n_0 \exp[-\varepsilon\bar{\varphi}_1(z)]/\langle \exp[-\varepsilon\bar{\varphi}_1(z)]\rangle. \tag{77}$$

A fluid theory expression for the wave equation for TG modes in a nonuniform plasma in a strong magnetic field can be found in the literature[5,7]

$$\frac{\partial}{\partial z}\alpha(z,\omega)\frac{\partial \delta\phi}{\partial z} + k_\perp^2 \delta\phi = 0, \tag{78}$$

where

$$\alpha(z,\omega) = \omega_{pz}^2(z)/\omega^2 - 1 \tag{79}$$

is a dielectric constant for the plasma and $\omega_{pz}(z)$ is the local plasma frequency, given by $\omega_{pz}(z) = \sqrt{4\pi q^2 n_{eq}(z)/m_q}$. A first order correction to the mode due to squeeze can then be obtained by using Eq. (77) in Eq. (78) and Taylor expanding in ε

$$\alpha_0(\omega)\frac{\partial^2 \delta\phi}{\partial z^2} + \varepsilon[\alpha_0(\omega)+1]\frac{\partial}{\partial z}(\langle\bar{\varphi}_1\rangle - \bar{\varphi}_1(z))\frac{\partial \delta\phi}{\partial z} + k_\perp^2\delta\phi = 0, \tag{80}$$

where

$$\alpha_0(\omega) = \omega_p^2/\omega^2 - 1 \tag{81}$$

is the z-independent unsqueezed value for α.

To zeroth-order in ε (i.e., for an unsqueezed plasma), the solution of Eq. (80) has modes of the form (cf. Eqs. (31), (45), and (55))

$$\delta\phi_0^m(z) = \cos[k_m(z+L/2)] \tag{82}$$

with frequencies satisfying

$$-k_m^2\alpha_0(\omega) + k_\perp^2 = 0. \tag{83}$$

Equation (83) can be solved for ω to yield the cold-fluid TG dispersion relation for unsqueezed frequency for mode m, ω_0^m

$$\omega_0^m = \omega_p k_m/\sqrt{k_m^2 + k_\perp^2}. \tag{84}$$

The first order correction to ω can be found by applying perturbation theory to Eq. (80). Let $\omega = \omega_0^m + \varepsilon\omega_1^m$, where ω_1^m is the first-order correction to the frequency. Also, let $\delta\phi(z) = \delta\phi_0^m(z) + \varepsilon\delta\phi_1^m(z)$, where $\delta\phi_1^m(z)$ is the first order correction to the eigenmode due to squeeze. Substituting these relations in Eq. (80) and Taylor expanding to first-order in ε yields, at first order

$$\omega_1^m\alpha_0'(\omega_0^m)\frac{\partial^2\delta\phi_0^m}{\partial z^2} + \alpha_0(\omega_0^m)\frac{\partial^2\delta\phi_1^m}{\partial z^2} + [\alpha_0(\omega_0^m)+1]\frac{\partial}{\partial z}(\langle\bar{\varphi}_1\rangle - \bar{\varphi}_1(z))\frac{\partial\delta\phi_0^m}{\partial z} + k_\perp^2\delta\phi_1^m = 0, \tag{85}$$

where the prime on α_0 in the first term denotes differentiation. If we multiply this equation by $\delta\phi_0^m(z)$ and integrate in z over the length of the plasma, we obtain

$$-\frac{L}{2}k_m^2\omega_1^m\alpha_0'(\omega_0^m) - k_m^2[\alpha_0(\omega_0^m)+1] \times \int_{-L/2}^{L/2} dz \sin^2[k_m(z+L/2)](\langle\bar{\varphi}_1\rangle - \bar{\varphi}_1(z)) = 0, \tag{86}$$

where we have integrated by parts and substituted for $\delta\phi_0^m(z)$ from Eq. (82). Note that on integration by parts the terms involving $\delta\phi_1^m$ vanish. Equation (86) can be simplified using the relation $\alpha_0'(\omega_0^m) = -2[\alpha_0(\omega_0^m)+1]/\omega_0^m$, which follows from Eq. (81). Substituting this into Eq. (86) yields the following expression for the first-order frequency shift due to squeeze:

$$\omega_1^m = \omega_0^m\frac{1}{L}\int_{-L/2}^{L/2} dz \sin^2[k_m(z+L/2)](\langle\bar{\varphi}_1\rangle - \bar{\varphi}_1(z)). \tag{87}$$

This result can be further simplified by substituting the Fourier expansion for $\bar{\varphi}_1(z)$ given in Eq. (17), and by using $k_m = m\pi/L$. Then the integral in Eq. (87) yields

$$\omega_1^m = \omega_0^m\frac{\varphi_m^1}{4T}, \tag{88}$$

where φ_m^1 is the mth Fourier cosine coefficient of the squeeze potential. This expression for the first order frequency shift due to squeeze agrees with the more general result given by Eq. (73) when that equation is evaluated in the cold-fluid regime, $K_m\lambda_D \ll 1$. This provides an independent check of

the general result. However, in one sense, Eq. (88) is more general than Eq. (73): Eq. (88) was derived from Eq. (87), which is valid for a squeeze of any functional form, not just a symmetric squeeze as was assumed in Eq. (73). In fact, Eq. (87) shows that only the z-symmetric (cosine) component of the squeeze potential contributes to the first-order frequency shift, since any odd (sine) component to the squeeze potential vanishes upon integration over z.

4. WKB fluid theory for $m \gg 1$

When the mode number m becomes sufficiently large, the Fourier component of the shielded squeeze potential $\bar{\varphi}^1_m$ becomes exponentially small, assuming that the squeeze is a smooth function of z. In this regime, Eq. (73) (or Eq. (88)) implies that the first order frequency shift due to squeeze is exponentially small and may therefore be negligible compared to the second-order shift. To find the shift in this regime, it is useful to apply WKB theory. For large m, $\delta\phi(z)$ varies rapidly compared to the squeeze, and can be determined using an eikonal approach where we write $\delta\phi(z) = \exp[S(z)]$. From Eq. (78), the eikonal $S(z)$ satisfies

$$\alpha[S'' + (S')^2] + S'\alpha' + k_\perp^2 = 0. \tag{89}$$

If we assume derivatives of S are of order $m \gg 1$ but the derivative of α is of order unity, the dominant balance in the equation is $\alpha(S')^2 = -k_\perp^2$ with solution

$$S \equiv S_0 = \pm ik_\perp \int^z dz/\sqrt{\alpha(z,\omega)}. \tag{90}$$

To next order in $1/m$, we rewrite Eq. (89) as

$$S' = \pm i\sqrt{k_\perp^2/\alpha + S'' + S'\alpha'/\alpha}. \tag{91}$$

Noting that the last two terms in the square root are small compared to the first, we replace S by S_0 in these two terms in order to obtain the next-order correction to S, S_1

$$\begin{aligned} S_1' &= \pm i\sqrt{k_\perp^2/\alpha + S_0'' + S_0'\alpha'/\alpha} \\ &= \pm i\sqrt{k_\perp^2/\alpha \mp ik_\perp\alpha'/2\alpha^{3/2} \pm ik_\perp\alpha'/\alpha^{3/2}} \\ &\simeq \pm i\frac{k_\perp}{\sqrt{\alpha}}\left[1 \pm \frac{i\alpha'}{4k_\perp\sqrt{\alpha}}\right], \end{aligned} \tag{92}$$

where we used Eq. (90) in the second step and Taylor-expanded the square root in the last step. Integrating in z, this yields

$$S_1 = S_0 - \frac{1}{4}\ln\alpha. \tag{93}$$

Substituting this eikonal into $\delta\phi(z) = \exp[S(z)]$ implies

$$\delta\phi(z) = [\alpha(z,\omega)]^{-1/4}\exp\left[\pm ik_\perp\int^z dz/\sqrt{\alpha(z,\omega)}\right]. \tag{94}$$

These two independent solutions for the mode potential must be combined to match the boundary conditions that the slope of the potential vanishes at both plasma ends, which implies

$$\delta\phi(z) = [\alpha(z,\omega)]^{-1/4}\cos\left[k_\perp\int_{-L/2}^{z} dz/\sqrt{\alpha(z,\omega)}\right], \tag{95}$$

where

$$k_\perp\int_{-L/2}^{L/2} dz/\sqrt{\alpha(z,\omega)} = m\pi. \tag{96}$$

This is the WKB dispersion relation for a given mode number m. To solve the dispersion relation, we substitute Eqs. (77) and (79) for α and Taylor expand in ε, obtaining

$$\begin{aligned} k_\perp\int_{-L/2}^{L/2} dz\frac{1}{\sqrt{\alpha_0(\omega)}}\Bigg[1 - \frac{\omega_p^2}{2\omega^2}\varepsilon\frac{\langle\bar{\varphi}_1\rangle - \bar{\varphi}_1}{\alpha_0(\omega)} \\ + \frac{\omega_p^2}{8\omega^2\alpha_0(\omega)}\varepsilon^2\left(3\frac{\omega_p^2}{\omega^2}\frac{(\langle\bar{\varphi}_1\rangle - \bar{\varphi}_1)^2}{\alpha_0(\omega)} - 2[(\langle\bar{\varphi}_1\rangle - \bar{\varphi}_1)^2\right. \\ \left. + \langle\bar{\varphi}_1\rangle^2 - \langle\bar{\varphi}_1^2\rangle]\right)\Bigg] = m\pi. \end{aligned} \tag{97}$$

Upon performing the integration, this becomes

$$\frac{k_\perp L}{\sqrt{\alpha_0(\omega)}}\left[1 + \frac{3}{8}\varepsilon^2\left(\frac{\omega_p^2}{\omega^2\alpha_0(\omega)}\right)^2[\langle\bar{\varphi}_1^2\rangle - \langle\bar{\varphi}_1\rangle^2]\right] = m\pi. \tag{98}$$

Squaring both sides and rearranging yields

$$k_m^2\alpha_0(\omega) = k_\perp^2\left[1 + \varepsilon^2\frac{3}{8}\left(\frac{\omega_p^2}{\omega^2\alpha_0(\omega)}\right)^2[\langle\bar{\varphi}_1^2\rangle - \langle\bar{\varphi}_1\rangle^2]\right]. \tag{99}$$

At $\mathcal{O}(\varepsilon^2)$ on the right hand side, we can replace $\alpha_0(\omega)$ and ω by their zeroth order unsqueezed values, given by Eqs. (83) and (84), obtaining

$$k_m^2\alpha_0(\omega) = k_\perp^2\left[1 + \frac{3}{4}\left(1 + \frac{k_m^2}{k_\perp^2}\right)^2\varepsilon^2[\langle\bar{\varphi}_1^2\rangle - \langle\bar{\varphi}_1\rangle^2]\right]. \tag{100}$$

Substituting on the left hand side $\omega = \omega_0^m + \varepsilon^2\omega_2^m$ and expanding, we obtain

$$-2k_m^2\frac{\omega_p^2}{(\omega_0^m)^3}\omega_2^m = \frac{3}{4}K_m^2\left(1 + \frac{k_m^2}{k_\perp^2}\right)[\langle\bar{\varphi}_1^2\rangle - \langle\bar{\varphi}_1\rangle^2],$$

which implies

$$\omega_2^m = -\frac{3\omega_0^m}{8}\left(1 + \frac{k_m^2}{k_\perp^2}\right)[\langle\bar{\varphi}_1^2\rangle - \langle\bar{\varphi}_1\rangle^2]. \tag{101}$$

Thus, for the regime $m \gg 1$ where the squeeze potential varies in z slowly compared to the mode wavelength, the frequency shift is always negative, and is second-order in the squeeze potential.

5. Mode damping at second order in ε

In Eq. (72), we observed that TG mode damping due to squeeze is exponentially small at first order in ε when the mode phase velocity is large. We must therefore work to second order in this regime. The second order dispersion relation is given by

$$\begin{aligned}&\mathbf{M}_0(\bar{\omega}_0^m).\mathbf{e}_2^m+\bar{\omega}_1^m\partial_{\bar{\omega}}\mathbf{M}_0(\bar{\omega}_0^m).\mathbf{e}_1^m\\&+\bar{\omega}_2^m\partial_{\bar{\omega}}\mathbf{M}_0(\bar{\omega}_0^m).\mathbf{e}_0^m+\frac{(\bar{\omega}_1^m)^2}{2}\partial_{\bar{\omega}}^2\mathbf{M}_0(\bar{\omega}_0^m).\mathbf{e}_0^m\\&+\mathbf{M}_1(\bar{\omega}_0^m).\mathbf{e}_1^m+\bar{\omega}_1^m\partial_{\bar{\omega}}\mathbf{M}_1(\bar{\omega}_0^m).\mathbf{e}_0^m+\mathbf{M}_2(\bar{\omega}_0^m).\mathbf{e}_0^m=0.\end{aligned}\tag{102}$$

We take the product of $(\mathbf{e}_0^m)^T$ and Eq. (102). As a result, the product of the first and second terms in Eq. (102) is zero and using Eq. (56) for $\mathbf{e}_0^m$ and Eq. (62) for $\mathbf{e}_1^m$ we have

$$\begin{aligned}&-\bar{\omega}_2^m\partial_{\bar{\omega}}M_0^{mm}(\bar{\omega}_0^m)\\&=\frac{(\bar{\omega}_1^m)^2}{\bar{\omega}^2}\partial_{\bar{\omega}}^2M_0^{mm}(\bar{\omega}_0^m)+\sum_{j\neq m}M_1^{mj}(\bar{\omega}_0^m).M_1^{jm}(\bar{\omega}_0^m)/M_0^{jj}(\bar{\omega}_0^m)\\&+\bar{\omega}_1^m\partial_{\bar{\omega}}M_1^{mm}(\bar{\omega}_0^m)+M_2^{mm}(\bar{\omega}_0^m).\end{aligned}\tag{103}$$

Now we take the imaginary part of above equation assuming that $\bar{\omega}_{0r}^m\gg m$, which implies $\bar{\omega}_0^m\cong\bar{\omega}_{0r}^m,\bar{\omega}_1^m,M_0^{mm}(\bar{\omega}_{0r})$, and $M_1^{mm}(\bar{\omega}_{0r})$ are real. As a result,

$$\begin{aligned}&-\bar{\gamma}_2^m\partial_{\bar{\omega}}\mathrm{Re}M_0^{mm}(\bar{\omega}_{0r}^m)\\&=\mathrm{Im}\left[M_2^{mm}(\omega_{0r}^m)\right]+\mathrm{Im}\left[\sum_{j\neq m}M_1^{mj}(\bar{\omega}_{0r}^m)M_1^{jm}(\bar{\omega}_{0r}^m)/M_0^{ij}(\bar{\omega}_{0r}^m)\right].\end{aligned}\tag{104}$$

From Eq. (B21), the first term on the right hand side of Eq. (104), in the limit $\bar{\omega}_0^m\gg m$, is given by

$$\mathrm{Im}\,M_2^{mm}(\bar{\omega}_{0r}^m)=\frac{16\pi}{\lambda_D^2K_m^2\sqrt{2\pi}}\sum_{n=1}^{\infty}\left(\frac{n}{\bar{\omega}_{0r}^m}\right)^3e^{-(\bar{\omega}_{0r}^m)^2/2n^2}(\alpha_m^n)^2,\tag{105}$$

where α_m^n is defined in Eq. (61). Thus, solving for $\bar{\gamma}_2^m$, we obtain

$$\begin{aligned}\bar{\gamma}_2^m=&-\frac{16m\pi\sum_{n>m}^{\infty}\left(\frac{n}{\bar{\omega}_{0r}^m}\right)^3e^{-(\bar{\omega}_{0r}^m)^2/2n^2}(\alpha_m^n)^2}{\mathrm{P}\int_{-\infty}^{\infty}\frac{ve^{-v^2/2}dv}{(\bar{\omega}_{0r}^m/m-v)^2}}\\&+\frac{\mathrm{Im}\left[\sum_{j\neq m}M_1^{mj}(\bar{\omega}_{0r}^m)M_1^{jm}(\bar{\omega}_{0r}^m)/M_0^{ij}(\bar{\omega}_{0r}^m)\right]}{\partial_{\bar{\omega}}\,\mathrm{Re}\,M_0^{mm}(\bar{\omega}_{0r}^m)}.\end{aligned}\tag{106}$$

The first term on the right hand side is the contribution to the damping rate due to the mth unsqueezed mode (cosine in position space). Particles slow down as they pass the squeeze and, thus, no longer see this mode as a simple cosine along their bounce orbits, as a function of their angle variables (which is proportional to time). As a result, the mth unsqueezed mode has nonzero Fourier terms in angle variable space. Particles with bounce frequency $\omega_b=\omega/n$ will resonantly interact with the nth Fourier term and, thus, enhance the damping rate of the mode. The lower bound of the sum in the numerator is $n>m$, since all the terms for which $1\leq n\leq m$ are exponentially small (assuming $\bar{\omega}_{0r}/m\gg1$).

Moreover, in the presence of a squeeze, the spatial form of the eigenmode is affected, see Fig. 1. Therefore, the shape of the mode potential is no longer a simple cosine in position space and consists of higher harmonics in z, which are all oscillating at the same frequency ω. The contribution to the damping rate given by the second term on the right hand side of Eq. (106) is due to the damping of these higher harmonics.

In Fig. 3, we compare the damping rate calculated from our computer simulations to the analytically calculated damping rates. Analytically calculated results, which are depicted as solid black curves, are evaluated from the sum of Eqs. (57), (71), and (106), up to second order in ε. The computer simulation results are depicted with squares.

For the lowest value of $\bar{\omega}_{0r}^1=4.56$, unsqueezed damping is large and becomes the dominant damping for values of $\varphi_s/T\lesssim0.25$. However, for $\varphi_s/T\gtrsim0.25$, squeeze damping with quadratic dependence on φ_s/T becomes larger than the unsqueezed damping rate. For $\bar{\omega}_{0r}^1=6.25,10.13,13.42$, and 20.03, unsqueezed damping is exponentially small. Thus, mode damping is only due to the presence of the squeeze and the damping rate has a quadratic dependence on φ_s/T.

As the amplitude of the squeeze potential φ_s/T approaches 1, the computer simulation results deviate from the analytically calculated damping rates which has a quadratic dependence behavior on $\varphi_{sq}^{\max}$. This is due to the fact that for larger φ_s/T, terms of order higher than $(\varphi_s/T)^2$ become significant and thus, these higher terms will be needed to more accurately evaluate the corrections to the eigenfrequencies and eigenmodes. Also, for larger φ_s/T, the population of particles trapped in the Debye shielded squeeze potential, which was not accounted for, becomes

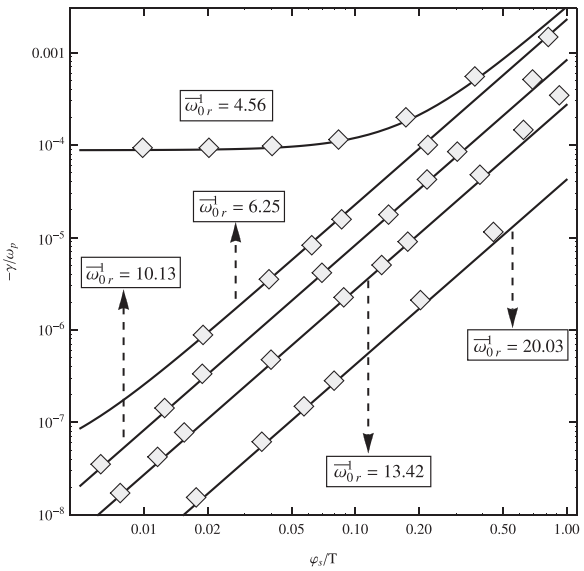

FIG. 3. Mode damping rate vs. size of the squeeze potential φ_s/T, for phase velocities: $\omega/k_1v_T=4.56,6.25,10.13,13.42$, and 20.03 for the mode $m=1$. Analytically calculated damping rates are shown in solid black lines. Computer simulation results are shown with diamonds.

larger and resonant trapped particle-wave interactions can become significant and further enhance the mode damping rate.

Figure 4 depicts the damping rate of the squeezed $m=1$ mode versus the Debye length. Solid curves are the analytically calculated results using the sum of Eqs. (57), (71), and (106), for squeeze potentials of value $\varphi_{sq}^{\max}/m_qL^2\omega_p^2 = 8.75\times10^{-6}$ and $\varphi_{sq}^{\max}/m_qL^2\omega_p^2 = 3.5\times10^{-5}$, which is 4 times larger than the former. The dashed line is the damping rate of the unsqueezed mode given by Eq. (57) and diamonds are the damping rates evaluated using computer simulations. For Debye lengths such that $\bar{\omega}_0^1 \ll 5$, where $\bar{\omega}_0^1 = \omega_r/k_1v_T$, the two solid curves converge to the unsqueezed (dashed) curve. For Debye lengths for which $\bar{\omega}_0^1 \gtrsim 5$ the unsqueezed damping rate (dashed curve) goes to zero exponentially, whereas the squeezed damping rates (solid curves) are finite. There is an approximately 16 fold difference between the values of the damping rates (solid curves), for Debye lengths at which $\bar{\omega}_0^1 \gtrsim 5$. This shows the quadratic dependence on the applied squeeze potential expected for large $\bar{\omega}_0^1$'s.

At very low values of λ_D/L, the damping rate again begins to fall off exponentially as T decreases further. This is because the Debye shielded squeeze potential φ_1 is a smooth function of position and thus, Fourier coefficients of the Debye shielded squeeze potential, i.e., $\bar{\varphi}_n^1$, become exponentially small with growing n.[8] In the small λ_D/L limit, where $\bar{\omega}_{0r}^1 \gg 1$, $n \gg 1$ bounce harmonics are necessary in order to satisfy the resonance condition, $n\omega_b = \omega_{0r}^1$. The effect of these higher harmonics becomes exponentially small, since these terms depend on $\bar{\varphi}_n^1$'s with $n \gg 1$.

III. 1D VLASOV-POISSON COMPUTER SIMULATIONS

For our computer simulations, we discretized the 2D phase space (z,v_z) on a 2 dimensional grid (using the method of lines[9]). That is, the distribution is discretized as $f(z_j, v_k, t) = f_{j,k}(t)$ where

$$\begin{aligned} z_j &= j\Delta z - L/2, \quad j = 0,1,\ldots,M_z, \\ v_k &= (k+1/2)\Delta v, \quad k = -M_v - 1,\ldots,M_v, \end{aligned} \tag{107}$$

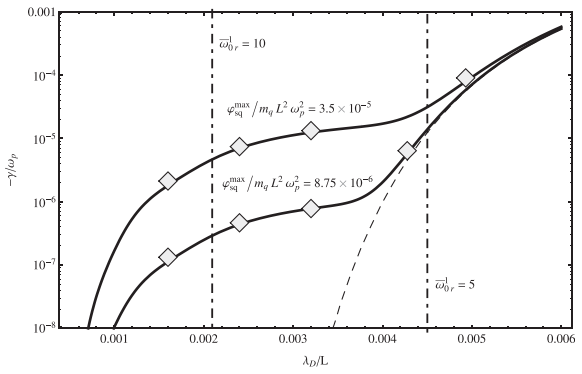

FIG. 4. Damping rate $(-\gamma/\omega_p)$ of mode $m=1$ versus Debye length (λ_D/L), depicted for constant squeeze potentials $\varphi_{sq}^{\max}/m_qL^2\omega_p^2 = 3.5\times10^{-5}$ (upper solid curve) and $\varphi_{sq}^{\max}/m_qL^2\omega_p^2 = 8.75\times10^{-6}$ (lower solid curve) in a plasma for which $k_\perp L = 15\pi$. The dashed curve depicts the unsqueezed Landau damping $(\varphi_{sq}=0)$. The dashed-dotted lines depict Debye lengths for which $\bar{\omega}_0^1 = 5$ and $\bar{\omega}_0^1 = 10$, where $\bar{\omega}_0^1 = \omega_r/k_1v_T$.

and where $\Delta z = L/M_z$, $\Delta v = V_{\max}/M_v$. The maximum velocity in the simulations is usually taken as $V_{\max} \simeq 8v_T$.

The condition of specular reflection at the plasma ends implies that $f(\pm L/2, v, t) = f(\pm L/2, -v, t)$ which translates to the grid as the boundary conditions

$$\begin{aligned} f_{0,k}(t) &= f_{0,-k-1}(t), \\ f_{M_z,k}(t) &= f_{M_z,-k-1}(t). \end{aligned} \tag{108}$$

We finite-difference the spatial and velocity derivatives in Eq. (3) using the centered difference method, obtaining

$$\begin{aligned} &\frac{\partial}{\partial t}f_{j,k}(t) + v_k\frac{f_{j+1,k}(t) - f_{j-1,k}(t)}{2\Delta z} \\ &\quad -\frac{1}{m_q}\left(\frac{\varphi_{j+1}(t) - \varphi_{j-1}(t)}{2\Delta z} + \frac{\partial}{\partial z}\varphi_{sq}(z)\right) \\ &\quad \times\frac{f_{j,k+1}(t) - f_{j,k-1}(t)}{2\Delta v} = 0. \end{aligned} \tag{109}$$

Poisson's equation, Eq. (5), is also finite-differenced and solved at each timestep using the FFT method.[10]

Time is advanced using the fourth order Runge-Kutta integration and each time step requires four plasma force evaluations.

For simulation of a squeezed plasma, the initial velocity distribution of plasma was Maxwellian. The squeezed equilibrium distribution function was obtained by gradually(adiabatically) turning on the squeeze potential over a time of order of 100 wave periods, in order to avoid launching unwanted modes.

For the initial condition of the squeezed mode damping simulation run, we add a perturbation to the squeezed equilibrium distribution $F_0(z,v)$

$$f(z,v;t=0) = F_0(z,v)(1+\delta\cos[k_1(z+L/2)]). \tag{110}$$

The difference between this initial perturbation from the exact $m=1$ mode is of the order φ_s/T. The largest contribution to the squeezed mode potential comes from the Fourier term $\cos[k_1(z+L/2)]$. (There are other contributions because our simulation is nonlinear.) We extract the $m_z=1$ Fourier component, $\delta\varphi_1(t)$, by integrating $\cos[k_z(z+L/2)]$ $\varphi_p(z,t)$ over z, where $\varphi_p(z,t)$ is the space charge potential. The damping rate γ and mode frequency ω are obtained by fitting the curve $\delta\varphi_1(t=0)e^{-\gamma t}\cos\omega t$ to $\delta\varphi_1(t)$. A typical result for $\delta\varphi_1(t)$ from our computer simulations is displayed in Fig. 5. The thick curve is the amplitude of the fitted function, which is exponentially decaying as a function of time.

IV. CYLINDRICALLY SYMMETRIC, R AND Z DEPENDENT SYSTEM

In order to make quantitative comparison between our theory and experimental results, we extend our 1D theory to a 2D system of axial(z) and radial(r) dependence. Figure 6 illustrates the confinement geometry for the rz system. The plasma is confined in a Malmberg-Penning trap consisting of a long conducting cylinder, axially divided into a number of sections. Radial confinement is provided by a strong uniform

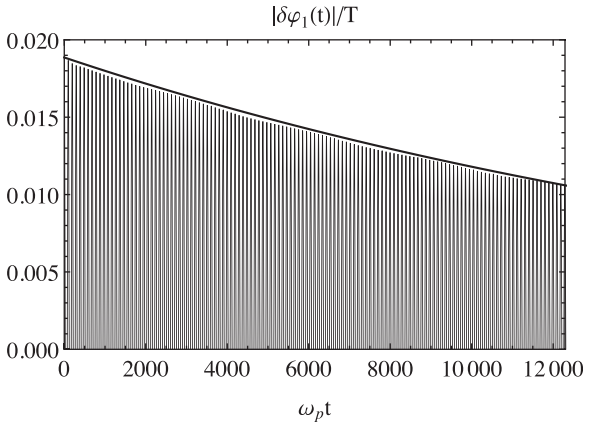

FIG. 5. The $m_z = 1$ Fourier component $\delta\varphi_1(t)$ of the space-charge potential $\varphi_p(z,t)$ and the exponentially damping amplitude $g(t) = 0.0188\exp[-4.7\times10^{-5}(\omega_p t)]$ (thick curve), obtained by fitting to $\delta\bar{\varphi}^1(t)$, as functions of time.

magnetic field **B** directed along the axis of cylinder. In this section, we assume an azimuthally symmetric perfectly conducting cylinder with radius r_w and extending axially from $-L/2$ to $L/2$, with L large compared to r_w. The squeeze potential is applied to a cylindrical section, which is centered at the axial midpoint of the cylinder and has a width Δ. We neglect effects involving the Debye sheath at the plasma ends, and simplify by assuming flat ends on the plasma at $z = \pm L/2$. Particles, which are traveling the length of the plasma along the magnetic field lines, are assumed to reflect specularly from the ends, as in Sec. II. The boundary conditions for the squeeze potential at the column ends are assumed for later convenience to be homogeneous Neumann conditions. Other homogeneous boundary conditions could have been used with negligible effect on our results, since the squeeze potential is applied at the axial center of a long column (see Fig. 6), so the squeeze potential is vanishingly small at the ends due to shielding by the plasma and the conducting walls. Neumann conditions simplify our expressions for the mode damping rate and frequency shift because the axial Fourier expansions for the mode potential and the squeeze potential then have a similar form.

The squeeze potential on the cylinder wall is taken to be

$$\begin{aligned}&\varphi(r_w,z) = 0 \quad -L/2 < z < -\Delta/2 \quad \text{or} \quad \Delta/2 < z < L/2,\\ &\varphi(r_w,z) = \varphi_{sq} \quad -\Delta/2 \le z \le \Delta/2.\end{aligned} \tag{111}$$

For a vacuum cylinder, we can calculate the potential inside the cylinder, with potential on the conducting walls of the trap given by Eq. (111). The vacuum potential φ_T satisfies the Laplace equation

$$\nabla^2\varphi_T = 0. \tag{112}$$

Standard Fourier analysis implies a solution of the form

$$\varphi_T(r,z) = \sum_{n=0}^{\infty} A_{2n} I_0(k_{2n} r)\cos[k_{2n}(z + L/2)], \tag{113}$$

where the Fourier coefficients A_{2n} are

$$\begin{aligned}A_{2n} &= \frac{2\varphi_{sq}}{LI_0(k_{2n}r_w)}\int_{-\Delta/2}^{\Delta/2}\cos[k_{2n}(z+L/2)]dz\\ &= \frac{2\varphi_{sq}}{k_{2n}LI_0(k_{2n}r_w)}2\sin[k_{2n}\Delta/2]\cos[k_{2n}L/2]\,,\end{aligned} \tag{114}$$

while for $n = 0$ term, we obtain

$$A_0 = \frac{\varphi_{sq}\Delta}{LI_0(0)}. \tag{115}$$

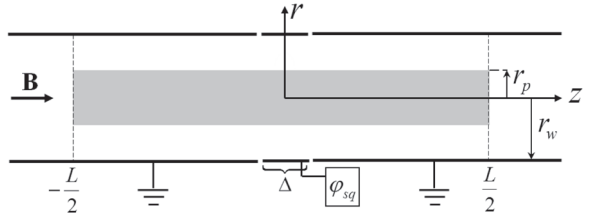

FIG. 6. Schematic depiction of the trap geometry and squeeze potential φ_{sq} applied to a cylindrical sector of width Δ. Other parts of the trap wall are grounded. Particles are assumed to reflect at the axial ends $z = \pm L/2$.

A. Plasma equilibrium: Unsqueezed and squeezed solutions

We assume the equilibrium plasma is a thermal equilibrium described by the Boltzmann distribution

$$\mathrm{F}_0(\mathbf{r},\mathbf{v}) = \frac{N\exp[-(H_0 + \omega_r p_\theta)/T]}{\int d\mathbf{r}d\mathbf{v}\exp[-(H_0+\omega_r p_\theta)/T]}, \tag{116}$$

where N is the total number of particles, ω_r is the plasma rotation frequency,

$$H_0 = \frac{m_q v^2}{2} + \varphi(\mathbf{r}), \tag{117}$$

and the potential $\varphi(\mathbf{r})$ is given by the sum of the vacuum potential $\varphi_T(\mathbf{r})$ and the potential due to plasma and its image on the conducting wall $\varphi_{pe}(\mathbf{r})$

$$\varphi(\mathbf{r}) = \varphi_T(\mathbf{r}) + \varphi_{pe}(\mathbf{r}). \tag{118}$$

The canonical angular momentum is given by

$$p_\theta = m_q v_\theta r + \frac{qB}{2c}r^2. \tag{119}$$

Substituting from Eqs. (118) and (119) in Eq. (116) after performing some algebra, we get

$$\mathrm{F}_0(\mathbf{r},\mathbf{v}) = n(r,z)\left(\frac{m_q}{2\pi T}\right)^{3/2}\exp\left[-\frac{m_q}{2T}(\mathbf{v}+\omega_r\hat{\theta})^2\right], \tag{120}$$

where the density is given by

$$n(r,z) = N\frac{\exp\left[-(\varphi_T+\varphi_{pe}+\varphi_c)/T\right]}{\int d\mathbf{r}\exp\left[-(\varphi_T+\varphi_{pe}+\varphi_c)/T\right]}, \tag{121}$$

and where $\varphi_c(r)$ is the radial confinement potential due to centrifugal force and magnetic field:

$$\varphi_c(r) = m_q\omega_r(\omega_c - \omega_r)r^2/2. \tag{122}$$

In order to calculate the space-charge potential φ_{pe}, we must solve the Poisson equation

$$\nabla^2\varphi_{pe}(r,z) = -4\pi q^2 n(r,z), \tag{123}$$

with the boundary condition given by $\varphi_{pe}(r_w,z) = 0$. We define the following dimensionless functions:

$$\begin{aligned}\chi(r,z) &= -\varphi_{pe}(r,z)/T,\\ \alpha(r) &= -\varphi_c(r)/T,\\ \beta(r,z) &= -\varphi_T(r,z)/T,\end{aligned} \tag{124}$$

and so rewrite Eq. (121) as

$$n(r,z) = N\frac{\exp[\chi+\alpha+\beta]}{\int d\mathbf{r}\exp[\chi+\alpha+\beta]}. \tag{125}$$

We will use the following averages:

$$\langle\ldots\rangle_z = \int_0^{r_w}\int_{-L/2}^{L/2} dz(\ldots)/L, \tag{126}$$

$$\langle\ldots\rangle_r = \int_0^{r_w} 2\pi r dr(\ldots)/2\pi r_w^2, \tag{127}$$

$$\langle\ldots\rangle_{rz} = \langle\langle\ldots\rangle_r\rangle_z. \tag{128}$$

We may then rewrite the Poisson equation (123) as

$$\nabla^2\chi(r,z) = \frac{4\pi q^2 N}{TV}\frac{\exp[\chi+\alpha+\beta]}{\langle\exp[\chi+\alpha+\beta]\rangle_{rz}}, \tag{129}$$

where $V = \pi r_w^2 L$. We expand the solution of Eq. (119) to first order in powers of the (scaled) squeeze potential $\beta(r,z)$, introducing the ordering parameter ε, as in Sec. II and writing the scaled plasma potential as a sum of the unsqueezed and squeezed terms

$$\chi = \chi_0 + \varepsilon\chi_1. \tag{130}$$

We then expand Eq. (129) to first order in ε

$$\begin{aligned}&\nabla^2\chi_0(r) + \varepsilon\nabla^2\chi_1(r,z)\\ &= \frac{4\pi q^2 N}{TV}\frac{\exp[\chi_0+\varepsilon\chi_1+\alpha+\varepsilon\beta]}{\langle\exp[\chi_0+\varepsilon\chi_1+\alpha+\varepsilon\beta]\rangle_{rz}}\end{aligned} \tag{131}$$

$$\approx \frac{4\pi q^2 N}{TV}\frac{e^{\chi_0+\alpha}}{\langle e^{\chi_0+\alpha}\rangle_r}\left(1+\varepsilon\chi_1+\varepsilon\beta - \frac{\varepsilon\langle(\chi_1+\beta)e^{\chi_0+\alpha}\rangle_{rz}}{\langle e^{\chi_0+\alpha}\rangle_r}\right). \tag{132}$$

Collecting powers of ε implies

$$\nabla^2\chi_0(r) = \frac{4\pi q^2 N}{TV}\frac{e^{\chi_0+\alpha}}{\langle e^{\chi_0+\alpha}\rangle_r}, \tag{133}$$

$$\nabla^2\chi_1(r,z) = \frac{4\pi q^2 N}{TV}\frac{e^{\chi_0+\alpha}}{\langle e^{\chi_0+\alpha}\rangle_r}\left(\chi_1+\beta - \frac{\langle(\chi_1+\beta)e^{\chi_0+\alpha}\rangle_{rz}}{\langle e^{\chi_0+\alpha}\rangle_r}\right). \tag{134}$$

Solving Eq. (133), we obtain the unsqueezed space-charge potential inside the plasma, $\chi_0(r)$. Equation (134) provides $\chi_1(r,z)$, the Debye-shielding response to the squeeze potential $\beta(r,z)$, similar to Eq. (9).

1. Unsqueezed equilibrium

The unsqueezed potential and density of a thermal equilibrium plasma was discussed in Ref. 11. The equilibrium Poisson equation (123) can be expressed as

$$\left(\frac{1}{\rho}\frac{\partial}{\partial\rho}\rho\frac{\partial}{\partial\rho}\right)\zeta = \exp(\zeta) - \gamma - 1, \tag{135}$$

where we defined the parameter γ and function ζ as

$$\gamma = 4\frac{\omega_r}{\omega_p^2}(\omega_c - \omega_r) - 1, \tag{136}$$

$$\zeta(\rho) = \chi_0(\rho) - \chi_0(0) + \alpha(\rho), \tag{137}$$

$\omega_p^2 = 4\pi e^2 n_0(0)/m$, $\rho = r/\lambda_D$, $\lambda_D = v_T/\omega_p$, and the density $n_0(r)$ is

$$n_0(r) = \frac{N}{V}\frac{e^{\chi_0+\alpha}}{\langle e^{\chi_0+\alpha}\rangle_r}. \tag{138}$$

Equation (135) is solved with boundary conditions

$$\zeta(0) = 0, \quad \partial_\rho\zeta|_{\rho=0} = 0. \tag{139}$$

The first boundary condition follows from Eq. (137). We can choose $\chi_0(0)$ so that the boundary condition $\chi_0(r_w) = 0$ is also satisfied. For a plasma with small Debye length compared to plasma radius, the plasma density and the potential inside the plasma are constant up to the vicinity of plasma radius where the density drops to zero in a distance of the order of λ_D. We define the plasma radius r_p as the radius where the density falls to $1/e$ of its value at the origin.[11] Figure 7 shows an example for an unsqueezed equilibrium, which is obtained

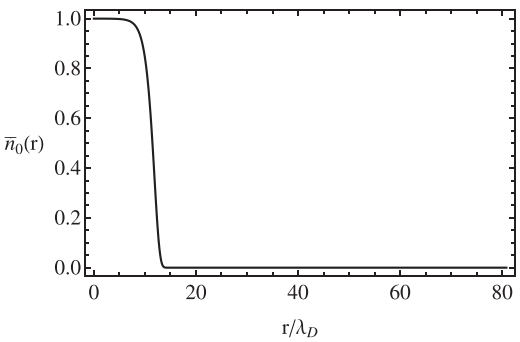

FIG. 7. Plot of the equilibrium density for a plasma with $T = 50\,\text{meV}$, $L = 10\,\text{cm}(L/\lambda_D = 282.6)$, $\omega_p = 1.263\times10^6\,\text{rad/s}$, $r_p \approx 0.42\,\text{cm}(r_p/\lambda_D \approx 11.87)$, $r_w = 2.86\,\text{cm}(r_w/\lambda_D = 80.83)$. Maximum density of the plasma at $r = 0$ is normalized to 1.

from numerically solving Eq. (135) with boundary conditions (139).

2. Squeezed equilibrium: A perturbative solution

We rewrite Eq. (134) as

$$\left(\frac{1}{\rho}\frac{\partial}{\partial\rho}\rho\frac{\partial}{\partial\rho}+\frac{\partial^2}{\partial\xi^2}\right)\chi_1(\rho,\xi) = \bar{n}_0(\rho)\left(\chi_1+\beta-\frac{\langle\bar{n}_0(\rho)(\chi_1+\beta)\rangle_{rz}}{\langle\bar{n}_0(\rho)\rangle_r}\right), \tag{140}$$

where $\bar{n}_0(\rho)=n_0(\rho)/n_0(0)$ is the scaled unsqueezed density profile, and $\xi=z/\lambda_D$. We will solve for $\chi_1(\rho,\xi)$ using the Galerkin method, as in Sec. I. From Eqs. (113) and (124), we write β as

$$\beta(\rho,\xi)=\sum_{n=1}^{\infty}R_n(\rho)\cos\left[\kappa_{2n}\left(\xi+\frac{\Lambda}{2}\right)\right], \tag{141}$$

$$R_n(\rho)=-\frac{\varphi_{sq}}{T}\frac{I_0(\kappa_{2n}\rho)}{I_0(\kappa_{2n}\rho_w)}\frac{2(-1)^n}{n\pi}\sin[k_{2n}\Delta/2], \tag{142}$$

where $\rho_w=r_w/\lambda_D$, $\Lambda=L/\lambda_D$, $\kappa_n=\lambda_D k_n$, and we neglect the $n=0$ term in β as the constant term does not affect the solution. We expand χ_1 using a complete series representation in ρ and ξ as follows:

$$\chi_1(\rho,\xi)=\sum_{m=1}^{\infty}\sum_{n=1}^{\infty}A_{mn}\mathrm{J}_0\left(\frac{x_m}{\rho_w}\rho\right)\cos\left[\kappa_n\left(\xi+\frac{\Lambda}{2}\right)\right], \tag{143}$$

where x_m is the mth zero of J_0. Substituting from Eqs. (141) and (143) in Eq. (140), multiplying by $\cos[\kappa_{2l}(\xi+\Lambda/2)]$ and integrating from $-\Lambda/2$ to $\Lambda/2$ yields

$$\sum_{m=1}^{\infty}A_{m,2l}\left[-\left(\frac{x_m}{\rho_w}\right)^2-\kappa_{2l}^2-\bar{n}_0(\rho)\right]\mathrm{J}_0\left(\frac{x_m}{\rho_w}\rho\right)=\bar{n}_0(\rho)R_l(\rho). \tag{144}$$

Now we multiply both sides by $\rho\mathrm{J}_0(x_n\rho/\rho_w)$ and integrate from 0 to ρ_w to get

$$\left[\left(\frac{x_n}{\rho_w}\right)^2+\kappa_{2l}^2\right]\frac{\rho_w^2}{2}\mathrm{J}_1^2(x_n)A_{n,2l} + \sum_m A_{m,2l}\int_0^{\rho_w}\bar{n}_0(\rho)\mathrm{J}_0\left(\frac{x_n}{\rho_w}\rho\right)\mathrm{J}_0\left(\frac{x_m}{\rho_w}\rho\right)\rho d\rho = -\int_0^{\rho_w}\bar{n}_0(\rho)R_l(\rho)\mathrm{J}_0\left(\frac{x_n}{\rho_w}\rho\right)\rho d\rho. \tag{145}$$

This relation can be written in the form of a matrix equation for each axial Fourier number l

$$\mathbf{N}_l.\mathbf{A}_l=\mathbf{B}_l, \tag{146}$$

where

$$(\mathbf{A}_l)_n=A_{n,2l}, \tag{147}$$

$$(\mathbf{B}_l)_n=-\int_0^{\rho_w}\bar{n}_0(\rho)R_l(\rho)\mathrm{J}_0\left(\frac{x_n}{\rho_w}\rho\right)\rho d\rho, \tag{148}$$

$$(\mathbf{N}_l)_{n,m}=\left[\left(\frac{x_n}{\rho_w}\right)^2+\kappa_{2l}^2\right]\frac{\rho_w^2}{2}\mathrm{J}_1^2(x_n)\delta_{nm} + \int_0^{\rho_w}\bar{n}_0(\rho)\mathrm{J}_0\left(\frac{x_n}{\rho_w}\rho\right)\mathrm{J}_0\left(\frac{x_m}{\rho_w}\rho\right)\rho d\rho. \tag{149}$$

The solution for $A_{n,2l}$'s is given by

$$\mathbf{A}_l=(\mathbf{N}_l)^{-1}.\mathbf{B}_l. \tag{150}$$

Figure 8 is the contour plot of the difference between the squeezed equilibrium density and the unsqueezed equilibrium density as a function of the radial and axial positions for a plasma of $T=50\,\mathrm{meV}$, $L=10\,\mathrm{cm}(L/\lambda_D=282.6)$, $\omega_p=1.263\times10^6\,\mathrm{Rad/s}$, $r_p\approx0.42\,\mathrm{cm}\,(r_p/\lambda_D\approx11.87)$, $r_w=2.86\,\mathrm{cm}(r_w/\lambda_D=80.83)$, for a squeeze with $\Delta=2.86\,\mathrm{cm}$ and $\varphi_{sq}=0.1\mathrm{eV}$. The horizontal range of the plot shows the whole length of the plasma, whereas the vertical (radial) range of the plot covers the vicinity of the plasma surface, since the change in the density due to squeeze potential is maximum close to the surface of plasma and goes exponentially to zero radially, from the surface towards the axis of plasma ($r=0$). To obtain this solution, 200 radial (Bessel) terms and 13 axial Fourier terms were used.

B. Squeezed linear modes

We now obtain the linear TG modes of the squeezed equilibrium. The method is similar to that used for 1D case, the difference being that there is now radial dependence. The linearized Vlasov equation in the presence of the squeeze is given by

$$\partial_t\delta\mathrm{f}+v\partial_z\delta\mathrm{f}-\partial_z(\varphi_0+\varepsilon\varphi_1)/m_q\partial_v\delta\mathrm{f}-\partial_z\delta\varphi/m_q\partial_v\mathrm{F}_0=0. \tag{151}$$

Here, φ_0 is the unsqueezed equilibrium potential, which is the sum of the centrifugal potential and the unsqueezed

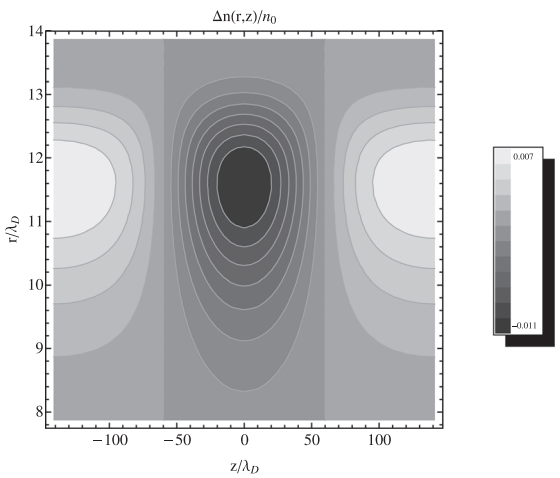

FIG. 8. Contour plot of the difference between the squeezed equilibrium density and the unsqueezed equilibrium density (the latter is the same as Fig. 7) as a function of the radial and axial positions for a plasma, for a squeeze with $\Delta=2.86\,\mathrm{cm}$ and $\varphi_{sq}=0.1\mathrm{eV}$.

space-charge potential of the plasma, and φ_1 is the Debye shielded squeeze potential

$$\varphi_0(r) = -T[\chi_0(r) - \chi_0(0) + \alpha(r)], \tag{152}$$

$$\varphi_1(r,z) = -T[\chi_1(r,z) + \beta(r,z)], \tag{153}$$

where α, β, χ_0 and χ_1 were obtained in the last section. The squeezed thermal equilibrium distribution $F_0(r,z,v)$ is given by Eq. (120). Using Eqs. (124), (129), (152), and (153), we can write $F_0(r, z,v)$ as

$$F_0(r,z,v) = n_0(0)\left(\frac{m_q}{2\pi T}\right)^{1/2} \times \frac{\bar{n}_0(r)e^{-\varepsilon\varphi_1/T}}{\langle \bar{n}_0(r)e^{-\varepsilon\varphi_1/T}\rangle_{rz}/\langle \bar{n}_0(r)\rangle_r}\exp\left[-\frac{m_q v^2}{2T}\right], \tag{154}$$

where $n_0(0)$ is the unsqueezed density at $r=0$ and $\bar{n}_0(r) = e^{-\varphi_0(r)/T}$ is the unsqueezed density profile normalized by its maximum value, $n_0(0)$. As in Sec. II, we solve Eq. (151) as an expansion in ε, i.e., assuming the height of the Debye shielded squeeze potential is small compared to temperature: $[\varphi_1(r,0) - \varphi_1(r,L/2)]/T \ll 1$. We define the scaled potential function $\bar{\varphi}_1$ and the scaled energy variable u as

$$\bar{\varphi}_1(r,z) = [\varphi_1(r,z) - \varphi_1(r,L/2)]/T, \tag{155}$$

$$u = m_q v^2/2T + \varepsilon\bar{\varphi}_1(r,z). \tag{156}$$

The reason we defined the function $\bar{\varphi}_1$ is that the bounce frequency and action of an unperturbed orbit of a particle at a radius r are functionals of the difference of the Debye shielded squeeze potential from its absolute minimum at that radius, which is defined by $\bar{\varphi}_1$. At a given radius r inside the plasma, trapped particles and passing particles have scaled energy u such that $0 < u < \varepsilon\bar{\varphi}_1(r,z)$ and $u > \varepsilon\bar{\varphi}_1(r,z)$, respectively. Figure 9 shows the Debye shielded, scaled squeeze potential $\bar{\varphi}_1(r,z)$, as a function of z, for radii $r = r_p, r = 0.9r_p$ and $r = 0.75r_p$, for the same parameters as Figs. 7 and 8. This shows the squeeze potential height dropping exponentially from the plasma surface towards the inner plasma.

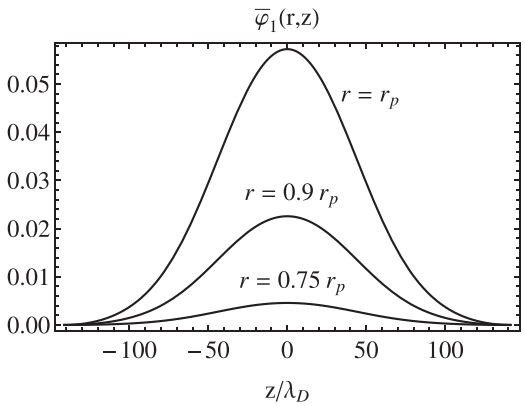

FIG. 9. Plot of the scaled Debye shielded squeeze potential $\bar{\varphi}_1(r,z)$ as a function of the axial position, at radii $r = r_p$, $0.9\,r_p$, and $0.75\,r_p$, for a plasma with the same parameters as Fig. 7.

The distribution F_0 can be rewritten in terms of u as

$$F_0(r,z,u) = n_0(0)\left(\frac{m_q}{2\pi T}\right)^{1/2} \frac{\bar{n}_0(r)e^{-\varepsilon\varphi_1(r,L/2)/T}}{\langle \bar{n}_0(r)e^{-\varepsilon\varphi_1(r,z)/T}\rangle_{rz}/\langle \bar{n}_0(r)\rangle_r} e^{-u}. \tag{157}$$

In order to solve Eq. (141), we again introduce action-angle variables for axial particle motion in the equilibrium potential

$$I(r,u;\varepsilon) = \frac{1}{2\pi}\oint p_z dz = \frac{m_q v_T}{2\pi}\oint\sqrt{2[u - \varepsilon\bar{\varphi}_1(r,z)]}dz, \tag{158}$$

$$\psi(r,z,u;\varepsilon) = \omega_b\int_{z_0}^{z}\frac{dz'}{v(r,z',u;\varepsilon)}, \tag{159}$$

$$\tau(r,u;\varepsilon) = \frac{2\pi}{\omega_b} = \oint\frac{dz}{v_T\sqrt{2[u - \varepsilon\bar{\varphi}_1(r,z)]}}. \tag{160}$$

As in Sec. II, the angle variable $\psi(r,z,u;\varepsilon)$ can be shown to have the functional form $\psi = \psi(r,z,\varepsilon/u)$

$$\psi = \frac{2\pi}{\oint\frac{dz'}{\sqrt{1-\varepsilon\bar{\varphi}_1(r,z')/u}}}\int_{z_0}^{z}\frac{dz'}{\sqrt{1-\varepsilon\bar{\varphi}_1(r,z')/u}} = \psi(r,z,\varepsilon/u), \tag{161}$$

and this equation can be inverted to yield the position versus the angle variable

$$z = z(r,\psi,\varepsilon/u), \tag{162}$$

where z is a periodic function of ψ. We can now write the Vlasov equation in terms of (r,ψ,I) as

$$\partial_t\delta f + \omega_b\partial_\psi\delta f - \partial_\psi\delta\varphi\partial_I F_0 = 0. \tag{163}$$

We expand the mode potential in a complete series in r and z, using the same Neumann conditions at the plasma ends, as in Sec. II B, assuming $\omega \ll \omega_p$ [see Eq. (31)]

$$\delta\varphi(r,z,t) = \sum_{l=1}\sum_{m=1}(\delta\phi_{lm}e^{-i\omega t} + \delta\phi_{lm}^* e^{i\omega t}) \times J_0\left(\frac{x_l}{r_w}r\right)\cos[k_m(z+L/2)]. \tag{164}$$

A particle at radius r and action $I(r,u;\varepsilon)$ follows an unperturbed orbit which is periodic in angle variable ψ. Therefore, we can write

$$\cos[k_m(z(r,\psi,u/\varepsilon)+L/2)] = \sum_{n=-\infty}^{\infty} C_m^n(r,\varepsilon/u)e^{in\psi}, \tag{165}$$

where the Fourier connection coefficients C_m^n are again given by Eq. (26), but are now functions of r through the action-angle transformation

$$C_m^n(r,\varepsilon/u) = \int_0^{2\pi}\frac{d\psi}{2\pi}\cos[k_m(z(r,\psi,u/\varepsilon)+L/2)]e^{-in\psi}. \tag{166}$$

Using Eq. (165), we can write Eq. (164) as

$$\delta\varphi(r;\psi,\varepsilon/u) = \sum_{l=1}\sum_{m=1}(\delta\phi_{lm}e^{-i\omega t} + \delta\phi^*_{lm}e^{i\omega t}) \times \mathrm{J}_0\left(\frac{x_l}{r_w}r\right)\sum_{n=-\infty}^{\infty} C^n_m(r,\varepsilon/u)e^{in\psi}. \quad (167)$$

As in Sec. II, δf and $\delta\varphi$ can be written in terms of Fourier series as

$$\delta\mathrm{f}(r,\psi,\varepsilon/u) = \sum_{n=-\infty}^{\infty}\delta f_n(r,\varepsilon/u)\exp[i(n\psi-\omega t)] + c.\mathrm{c}., \quad (168)$$

$$\delta\varphi(r,\psi,\varepsilon/u) = \sum_{n=-\infty}^{\infty}\delta\varphi_n(r,\varepsilon/u)\exp[i(n\psi-\omega t)] + c.c., \quad (169)$$

but $\delta\varphi_n(r,\varepsilon/u)$ now has an auxiliary radial expansion in terms of Bessel functions

$$\delta\varphi_n(r,\varepsilon/u) = \sum_{l=1}\sum_{m=1}\delta\phi_{lm}C^n_m(r,\varepsilon/u)\mathrm{J}_0\left(\frac{x_l}{r_w}r\right). \quad (170)$$

Substituting Eq. (168) in Eq. (163), we obtain

$$-\omega\delta f_n + n\omega_b\delta f_n + n\omega_b\delta\varphi_n\mathrm{F}_0/T = 0, \quad (171)$$

where we used $\partial_I\mathrm{F}_0 = (du/dI)\partial_u\mathrm{F}_0 = -\frac{\omega_b}{T}\mathrm{F}_0$. Solving for δf_n yields

$$\delta f_n(r,\varepsilon/u) = \frac{\omega_b\delta\varphi_n\mathrm{F}_0/T}{\omega/n-\omega_b}. \quad (172)$$

The mode potential and mode distribution function satisfy the linearized Poisson equation

$$\left(\frac{1}{r}\partial_r r\partial_r + \partial_z^2\right)\delta\varphi = -4\pi q^2\int_{-\infty}^{\infty}\delta\mathrm{f}dv. \quad (173)$$

Substituting Eq. (164) in Eq. (173), multiplying both sides by $2\cos[k_{\bar m}(z+L/2)]/L$ and integrating over z from $-L/2$ to $L/2$ yields

$$\sum_{l=1}\delta\phi_{l\bar m}\left[\left(\frac{x_l}{r_w}\right)^2 + k^2_{\bar m}\right]\mathrm{J}_0\left(\frac{x_l}{r_w}r\right)\mathrm{e}^{-\mathrm{i}\omega t} = 4\pi q^2\frac{2}{L}\int_{-\infty}^{\infty}\int_{-L/2}^{L/2}\delta\mathrm{f}\cos[k_{\bar{\mathrm{m}}}(z+L/2)]dzdv. \quad (174)$$

As in Sec. II, we can use the canonical variables (ψ,I) instead of (z,v), since $dzdp_z = d\psi dI = (T/\omega_b)dud\psi$. Applying Eqs. (168), (172), and (170) to Eq. (174), we obtain

$$\sum_{l=1}\delta\phi_{l\bar m}\left[\left(\frac{x_l}{r_w}\right)^2 + k^2_{\bar m}\right]\mathrm{J}_0\left(\frac{x_l}{r_w}r\right) = \frac{4\pi q^2}{L}\sum_{l=1}\sum_{m=1}\delta\phi_{lm}\mathrm{J}_0\left(\frac{x_l}{r_w}r\right)\sum_{n=-\infty}^{\infty}\int_0^{\infty}C^n_m(r,\varepsilon/u) \times C^{-n}_{\bar m}(r,\varepsilon/u)\frac{\mathrm{F}_0}{\omega/n-\omega_b}du. \quad (175)$$

Now we multiply both sides by $r\mathrm{J}_0(\frac{x_{\bar l}}{r_w}r)$ and integrate from 0 to r_w. The result is

$$\delta\phi_{\bar l\bar m} = \sum_{l=1}\sum_{m=1}\delta\phi_{lm}\frac{\frac{4\pi q^2}{L}\int_0^{r_w}r\mathrm{J}_0\left(\frac{x_l}{r_w}r\right)\mathrm{J}_0\left(\frac{x_{\bar l}}{r_w}r\right)\sum_{n=-\infty}^{\infty}\int_0^{\infty}C^n_m(r,\varepsilon/u)C^{-n}_{\bar m}(r,\varepsilon/u)\frac{\mathrm{F}_0}{\omega/n-\omega_\mathrm{b}}dudr}{\left[\left(\frac{x_{\bar l}}{r_w}\right)^2 + k^2_{\bar m}\right]\frac{r_w^2}{2}\mathrm{J}_1^2(\mathrm{x}_{\bar l})}. \quad (176)$$

Equation (176) is in the form of a tensor eigenvalue equation

$$M^{\bar l l\bar m m}\delta\phi_{lm} = 0, \quad (177)$$

where

$$M^{\bar l l\bar m m} = \delta_{\bar l l}\delta_{\bar m m} - \frac{\frac{4\pi q^2}{L}\int_0^{r_w}r\mathrm{J}_0\left(\frac{x_l}{r_w}r\right)\mathrm{J}_0\left(\frac{x_{\bar l}}{r_w}r\right)\sum_{n=-\infty}^{\infty}\int_0^{\infty}C^n_m(r,\varepsilon/u)C^{-n}_{\bar m}(r,\varepsilon/u)\frac{\mathrm{F}_0}{\omega/n-\omega_b}dudr}{\left[\left(\frac{x_{\bar l}}{r_w}\right)^2 + k^2_{\bar m}\right]\frac{r_w^2}{2}\mathrm{J}_1^2(x_{\bar l})}. \quad (178)$$

Since we assumed the squeeze to be symmetric with respect to the cylinder, we have $C^n_m = C^{-n}_m$. Moreover, we assume the trapped particle population is negligible compared to passing particles, therefore, we set the lower limit of the integral on u in Eq. (176) to be the height of the Debye shielded squeeze potential at radius r, i.e., $\varepsilon\bar\varphi_1(r,0)$. Introducing the scaled bounce frequency $\bar\omega_b(r,u) = \omega_b/k_1v_T$ and using Eq. (157) for the thermal equilibrium distribution F_0, we rewrite Eq. (178) as

$$M^{\bar{l}\bar{l}\bar{m}m} = \delta_{\bar{l}\bar{l}}\delta_{\bar{m}m} - \frac{\frac{8}{\sqrt{2\pi}\lambda_D^2}\int_0^{r_w} rdr \mathrm{J}_0\left(\frac{x_l}{r_w}r\right)\mathrm{J}_0\left(\frac{x_{\bar{l}}}{r_w}r\right)\bar{n}_0(r)e^{-\varepsilon\varphi_1(r,L/2)/T}\sum_{n=1}^{\infty}\int_{\varepsilon\bar{\varphi}_1(r,0)}^{\infty} du \frac{\bar{\omega}_b e^{-u}}{(\bar{\omega}/n)^2-\bar{\omega}_b^2} C_m^n\left(r,\frac{\varepsilon}{u}\right)C_{\bar{m}}^n\left(r,\frac{\varepsilon}{u}\right)}{\left\langle \frac{\bar{n}_0(r)}{\langle \bar{n}_0(r)\rangle_r} e^{-\varepsilon\varphi_1(r,z)/T}\right\rangle_{rz}\left[\left(\frac{x_{\bar{l}}}{r_w}\right)^2 + k_{\bar{m}}^2\right]\frac{r_w^2}{2}\mathrm{J}_1^2(x_{\bar{l}})}, \quad (179)$$

where $\bar{\omega} = \bar{\omega}_r + i\bar{\gamma}$ is the complex eigenfrequency ω scaled to $k_1 v_T$.

C. Perturbation method

Just as for Sec. I, the linear dispersion relation (177) can be written in matrix form

$$\mathbf{M}(\bar{\omega}).\mathbf{e} = 0, \quad (180)$$

where $\mathbf{e}$ is an eigenvector of the nullspace of $\mathbf{M}$ defined as

$$(\mathbf{e})^{lm} = \delta\phi_{lm}, \quad (181)$$

and $(\mathbf{M})^{\bar{l}\bar{l}\bar{m}m} = M^{\bar{l}\bar{l}\bar{m}m}$ [see Eq. (178)].

We again expand the matrix $\mathbf{M}$, the eigenfrequency $\bar{\omega}$ and eigenvector $\mathbf{e}$ in ε as in Eqs. (47)–(49). The resulting matrices $\mathbf{M}_0$, $\mathbf{M}_1$ and $\mathbf{M}_2$ are derived in Appendix C. For example, the zeroth-order (unsqueezed) matrix has components

$$M_0^{\bar{l}\bar{l}\bar{m}m} = \delta_{\bar{m}m}\left(\delta_{\bar{l}\bar{l}} + 2\mathrm{W}(\bar{\omega}/m)\frac{\int_0^{r_w} r\, dr\bar{n}_0(r)\mathrm{J}_0(x_{\bar{l}}r/r_w)\mathrm{J}_0(x_l r/r_w)}{\lambda_D^2[x_l^2 + k_m^2 r_w^2]\mathrm{J}_1^2(x_l)}\right). \quad (182)$$

1. Zeroth order in ε

The zeroth order dispersion relation for an unsqueezed plasma column is satisfied by mode $\mu = (n_r, m)$, where n_r and m are the radial and the axial mode numbers, respectively. The dispersion relation is given by

$$\mathbf{M}_0(\bar{\omega}_0^\mu)\cdot\mathbf{e}_0^\mu = 0. \quad (183)$$

From Eq. (183) and Eq. (182), we obtain the unsqueezed eigenvector $(\mathbf{e}_0^\mu)$ and eigenfrequency $\bar{\omega}_0^\mu$. We can write Eq. (183) explicitly as

$$(\mathbf{e}_0^\mu)^{\bar{l}m} = -\sum_{l'=1}^{\infty}(\mathbf{e}_0^\mu)^{l'm}\mathrm{W}(\bar{\omega}_0^\mu/m)\frac{\int_0^{r_w} rdr\mathrm{J}_0\left(\frac{x_{l'}}{r_w}r\right)\mathrm{J}_0\left(\frac{x_{\bar{l}}}{r_w}r\right)\bar{n}_0(r)}{\lambda_D^2\left[\left(\frac{x_{\bar{l}}}{r_w}\right)^2 + k_m^2\right]\frac{r_w^2}{2}\mathrm{J}_1^2(x_{\bar{l}})}. \quad (184)$$

This equation is only dependent on a single axial Fourier index m, while there is coupling between radial Bessel indices related to l' and $\bar{l}$. In other words, eigenmode $\mu = (n_r, m)$ is proportional to a single cosine function $\cos[k_m(z + L/2)]$ and a series in Bessel functions $\mathrm{J}_0(\frac{x_{l'}}{r_w}r)$ with $l' = 1, 2, \ldots$

$$\delta\phi_0^\mu(r,z) = |\delta\phi^\mu|\mathrm{R}_\mu(\mathrm{r})\cos[k_m(z + L/2)], \quad (185)$$

where

$$\mathrm{R}_\mu(r) = \sum_{l'=1}^{\infty}\frac{(\mathbf{e}_0^\mu)^{l'm}}{|\delta\phi^\mu|}\mathrm{J}_0\left(\frac{x_{l'}}{r_w}r\right). \quad (186)$$

Here, $|\delta\phi^\mu|$ is the arbitrary linear mode amplitude and $\mathrm{R}_\mu(r)$ are normalized so that $\mathrm{R}_\mu(0) = 1$. Eigenfrequencies $\bar{\omega}_0^\mu$ and the radial dependence of the unsqueezed eigenmodes ($(\mathbf{e}_0^\mu)^{l'm}$'s) are obtained by solving Eq. (184) as follows. We can rewrite the dispersion relation (184) as

$$-(\mathrm{W}(\bar{\omega}_0^\mu/m))^{-1}\mathrm{I}.(\mathbf{e}_0^\mu)^m = Q_{mm}.(\mathbf{e}_0^\mu)^m,$$
$$(Q_{mm})_{\bar{l}l'} = \frac{\int_0^{r_w} rdr\mathrm{J}_0\left(\frac{x_{l'}}{r_w}r\right)\mathrm{J}_0\left(\frac{x_{\bar{l}}}{r_w}r\right)\bar{n}_0(r)}{\lambda_D^2\left[\left(\frac{x_{\bar{l}}}{r_w}\right)^2 + k_m^2\right]\frac{r_w^2}{2}\mathrm{J}_1^2(x_{\bar{l}})}, \quad (187)$$

where I is the unit matrix. Thus, eigenvectors of the matrix Q_{mm} also satisfy the dispersion relation in Eq. (184). From the eigenvalue λ_μ of matrix Q_{mm}, we obtain the related eigenfrequency $\bar{\omega}_0^\mu$ via inversion

$$\bar{\omega}_0^\mu = m\mathrm{W}^{-1}(-\lambda_\mu^{-1}), \quad (188)$$

where W^{-1} is the inverse of the function W.

An alternative description of unsqueezed modes can be obtained from Eq. (184), (also from Eqs. (151) and (173) setting $\varphi_1 = 0$): the radial part of the eigenmode μ, i.e., $\mathrm{R}_\mu(r)$ satisfies

$$\left[-\nabla_r^2 + k_m^2 + \lambda_D^{-2}\mathrm{W}\left(\frac{\bar{\omega}_0^\mu}{m}\right)\bar{n}_0(r)\right]\mathrm{R}_\mu(r) = 0, \quad (189)$$

where $\nabla_r^2 = \frac{1}{r}\partial_r r\partial_r$. We can show that modes $\mu = (n_r, m)$ and $\mu' = (n'_r, m)$, which have the same axial mode number

m and different radial mode numbers n_r and n_r', are orthogonal with respect to the inner product $\int_0^{r_w} \bar{n}_0(r) r dr(\ldots)$. For the functions R_μ and R_μ', we can write

$$\left[-\nabla_r^2 + k_m^2 + \lambda_D^{-2}\mathrm{W}\left(\frac{\bar{\omega}_0^\mu}{m}\right)\bar{n}_0(r)\right]\mathrm{R}_\mu(r) = 0, \tag{190}$$

$$\left[-\nabla_r^2 + k_m^2 + \lambda_D^{-2}\mathrm{W}\left(\frac{\bar{\omega}_0^{\mu'}}{m}\right)\bar{n}_0(r)\right]\mathrm{R}_{\mu'}(r) = 0. \tag{191}$$

Multiplying Eq. (190) by $r\mathrm{R}_{\mu'}(\mathrm{r})$ and Eq. (191) by $r\mathrm{R}_\mu(\mathrm{r})$, subtracting Eq. (191) from Eq. (190) and integrating from 0 to r_w we get

$$\lambda_D^{-2}\left[\mathrm{W}\left(\frac{\bar{\omega}_0^\mu}{m}\right) - \mathrm{W}\left(\frac{\bar{\omega}_0^{\mu'}}{m}\right)\right]\int_0^{r_w} \bar{n}_0(r)\mathrm{R}_\mu(r)\mathrm{R}_{\mu'}(r) r dr$$
$$= \int_0^{r_w} dr\partial_r\left(r\mathrm{R}_\mu(r)\partial_r\mathrm{R}_{\mu'}(r) - r\mathrm{R}_\mu(r)\partial_r\mathrm{R}_\mu(r)\right) = 0. \tag{192}$$

In the above equation, the right hand side is zero since $\mathrm{R}(r)$'s are zero at the wall. Thus, we arrive at the following orthonormality condition:

$$\int_0^{r_w} \bar{n}_0(r)\mathrm{R}_\mu(r)\mathrm{R}_{\mu'}(r) r dr = \delta_{l,l'}\int_0^{r_w} \bar{n}_0(r)[\mathrm{R}_\mu(r)]^2 r dr. \tag{193}$$

In a similar way, we can show $\mathrm{W}(\frac{\bar{\omega}_0^\mu}{m})$ is real. Assuming $\bar{\omega}_0^\mu$ and $\mathrm{R}_\mu(r)$ to be complex, we have

$$\left[-\nabla_r^2 + k_m^2 + \lambda_D^{-2}\mathrm{W}\left(\frac{\bar{\omega}_0^\mu}{m}\right)\bar{n}_0(r)\right]\mathrm{R}_\mu(r) = 0, \tag{194}$$

$$\left[-\nabla_r^2 + k_m^2 + \lambda_D^{-2}\left(\mathrm{W}\left(\frac{\bar{\omega}_0^\mu}{m}\right)\right)^*\bar{n}_0(r)\right]\mathrm{R}_\mu^*(r) = 0. \tag{195}$$

Multiplying Eq. (194) by $r\mathrm{R}_\mu^*(r)$ and Eq. (195) by $r\mathrm{R}_\mu(r)$, subtracting Eq. (195) from Eq. (194) and integrating from 0 to r_w, we get

$$\lambda_D^{-2}\left[\mathrm{W}\left(\frac{\bar{\omega}_0^\mu}{m}\right)^* - \left(\mathrm{W}\left(\frac{\bar{\omega}_0^\mu}{m}\right)\right)\right]\int_0^{r_w} \bar{n}_0(r)\mathrm{R}_\mu(r)\mathrm{R}_\mu^*(r)\mathrm{rdr}$$
$$= \int_0^{r_w} dr\partial_r\left(r\mathrm{R}_\mu(r)\partial_r\mathrm{R}_\mu^*(r) - r\mathrm{R}_\mu^*(r)\partial_r\mathrm{R}_\mu(r)\right) = 0. \tag{196}$$

In this equation, the right hand side is zero since $\mathrm{R}_\mu(r_w) = 0$. Also for the integral on the left hand side, we have

$$\int_0^{r_w} \bar{n}_0(r)\mathrm{R}_\mu(r)\mathrm{R}_\mu^*(r) r dr$$
$$= \int_0^{r_w} \bar{n}_0(r)(\mathrm{Re}[\mathrm{R}_\mu(r)]^2 + \mathrm{Im}[\mathrm{R}_\mu(r)]^2) r dr > 0, \tag{197}$$

which implies

$$\mathrm{W}\left(\frac{\bar{\omega}_0^\mu}{m}\right) = \left(\mathrm{W}\left(\frac{\bar{\omega}_0^\mu}{m}\right)\right)^*. \tag{198}$$

Using Eq. (198) in Eq. (195), we see that $\mathrm{R}_\mu(r)$ and $\mathrm{R}_\mu^*(r)$ satisfy the same equation. Thus, from the uniqueness of the solution of Poisson equation $\mathrm{R}_\mu(r)$ is also real, and therefore $\mathbf{e}_0^\mu$ is real.

Figure 10 shows the first three radial eigenvectors with axial mode number $m = 1$, $\mathrm{R}_{1,1}(r)$, $\mathrm{R}_{2,1}(r)$, and $\mathrm{R}_{3,1}(r)$. We evaluated the eigenfrequencies related to these modes using both the Galerkin method and the shooting method. For the Galerkin method, the matrix eigenvalue equation (187) is solved by keeping a finite number of Bessel terms (N_{Gal}), to construct the matrix Q_{11}. For the shooting method, the differential equation (189) with initial conditions $\partial_r\mathrm{R}_\mu(0) = 0$ and $\mathrm{R}_\mu(0) = 1$ is solved for an eigenfrequency and its related eigenmode which satisfy the wall boundary condition $\mathrm{R}_\mu(r_p) = 0$. Frequencies obtained from the Galerkin method ω_{Gal} and shooting method ω_{Sho} are compared in Table I. In the second column of the table, which gives the mode frequency obtained from Galerkin method with $N_{\mathrm{Gal}} = 20$, we see that mode $\mu = (n_r, m)$ with $n_r = 1$ and $m = 1$ is undamped $(\mathrm{Im}[\omega_{\mathrm{Gal}}/\omega_p] = -3.84 \times 10^{-35})$. Furthermore, the real part of its eigenfrequency is equal to the Trivelpiece-Gould mode frequency for a cold fluid plasma of the same parameters, obtained from Eq. (1) (see Table I). The real part of the eigenfrequencies becomes smaller with increasing radial mode number n_r. Furthermore, modes with higher radial mode number, i.e., $n_r = 2,3$, are heavily damped. The third and fourth column of Table I compare the frequencies obtained from the shooting method to frequencies obtained from Galerkin method with, respectively, $N_{\mathrm{Gal}} = 20$ and $N_{\mathrm{Gal}} = 50$ terms. By increasing the number of terms for the Galerkin method, frequencies obtained from the Galerkin method converge to the shooting method frequencies. The fifth column of the table gives the mode frequencies obtained from cold fluid theory with a top hat profile, evaluated using Eq. (1).

In order to describe the squeezed modes, we find it useful to note that the zeroth order dispersion tensor $\mathbf{M}_0$ has the following form:

$$\mathbf{M}_0 = \begin{pmatrix} \mathbf{M}_0^{11} & 0 & 0 & \ldots \\ 0 & \mathbf{M}_0^{22} & 0 & \ldots \\ 0 & 0 & \mathbf{M}_0^{33} & \ldots \\ \vdots & & & \end{pmatrix}, \tag{199}$$

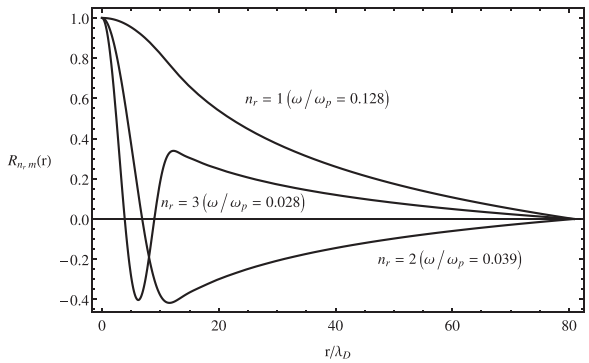

FIG. 10. Plot of the radial dependence of the modes $\mu = (n_r, m)$, with axial mode number $m = 1$ and three radial mode numbers $n_r = 1, 2, 3$, in an unsqueezed plasma with the same parameters as Fig. 7.

TABLE I. Frequencies of unsqueezed eigenmodes $\mu=(n_r,m)$: (1, 1), (2, 1), and (3, 1), where n_r is the radial and m is the axial mode numbers, for a plasma with the same parameters as Fig. 7. Frequencies $\omega_{\rm Gal}$ and $\omega_{\rm Sho}$ were obtained using the Galerkin method and the shooting method, respectively. $N_{\rm Gal}$ is the number of Bessel terms used to construct the dispersion matrix $\mathbf{M}_0^{ll}$.

Mode number (n_r,m)	$\omega_{\rm Gal}/\omega_p$ $N_{\rm Gal}=20$	$(\omega_{\rm Sho}-\omega_{\rm Gal})/\lvert\omega_{\rm Gal}\rvert$ $N_{\rm Gal}=20$	$(\omega_{\rm Sho}-\omega_{\rm Gal})/\lvert\omega_{\rm Gal}\rvert$ $N_{\rm Gal}=50$	$\omega_{\rm TG}/\omega_p$ From Eq. (1)
(1,1)	0.1285	$(4.1+i3.7)\times10^{-3}$	$(2.6+i2.4)\times10^{-6}$	0.1285
(2,1)	$0.0388-i1.08\times10^{-3}$	$(5.03+i1.1)\times10^{-4}$	$(9.5+i2.1)\times10^{-7}$	0.0316
(3,1)	$0.0281-i5.21\times10^{-3}$	2.3×10^{-5}	1.7×10^{-7}	0.0177

where $(\mathbf{M}_0^{\bar{m}m})^{l\bar{l}}=M_0^{\bar{l}l\bar{m}m}$ and $M_0^{\bar{l}l\bar{m}m}$ is given by Eq. (182). The mth unsqueezed eigenvector $(\mathbf{e}_0^\mu)^m$ satisfies

$$\mathbf{M}_0^{mm}(\bar{\omega}_0^\mu).(\mathbf{e}_0^\mu)^m=0 \tag{200}$$

and has components $((\mathbf{e}_0^\mu)^m)^l=(\mathbf{e}_0^\mu)^{ml}$ (see Eqs. (83) and (84) and (183) and (184)). The explicit indices (mm) are related to the axial Fourier components, which are not coupled at zeroth order (hence the diagonal form of Eq. (199)).

The matrix $\mathbf{M}_0^{mm}$ (for axial mode m) has radial eigenvectors $(\mathbf{e}_0^\mu)^m$ and eigenfrequencies corresponding to unsqueezed TG modes, as shown in Fig. 10 (see Eq. (186)). The zeroth order damping rate, which is the Landau damping of the unsqueezed system, follows from the same argument as for our 1D model of Sec. II. Assuming $\bar{\omega}_0^\mu\gg\gamma_0^\mu$ and using the fact that $\mathrm{W}(\bar{\omega}_0^\mu/m)$ is real, a Taylor expansion of $\mathrm{Im}\,\mathrm{W}(\bar{\omega}_0^\mu/m)=0$ yields

$$\bar{\gamma}_0^\mu=-\frac{\pi\bar{\omega}_{0r}^\mu e^{-\frac{(\bar{\omega}_{0r}^\mu)^2}{2m^2}}}{\mathrm{P}\int_{-\infty}^{\infty}\frac{ve^{-v^2/2}dv}{(\bar{\omega}_{0r}^\mu/m-v)^2}}, \tag{201}$$

the same formula as for the 1D model of Sec. II, Eq. (59). Since $\bar{\gamma}_0^\mu$ is proportional to $e^{-(\bar{\omega}_0^\mu)^2/2m^2}$, in the regime where $\bar{\omega}_0^\mu\gg m$, the zeroth order damping rate is exponentially small.

We will also be using the left eigenvector $\hat{\mathbf{e}}_0^\mu$ of $\mathbf{M}_0(\bar{\omega}_0^\mu)$. The left eigenvectors differ from the right eigenvectors $\mathbf{e}_0^\mu$ because $\mathbf{M}_0^{mm}$ is not symmetric. The left eigenvectors satisfy

$$\hat{\mathbf{e}}_0^\mu.\mathbf{M}_0(\bar{\omega}_0^\mu)=0. \tag{202}$$

Using Eq. (182), we can write the above equation explicitly as

$$(\hat{\mathbf{e}}_0^\mu)^{\bar{l}m}=-\sum_{l'=1}^{\infty}(\hat{\mathbf{e}}_0^\mu)^{l'm}\mathrm{W}(\bar{\omega}_0^\mu/m)\times\frac{\int_0^{r_w}rdr\mathrm{J}_0\left(\frac{x_{l'}}{r_w}r\right)\mathrm{J}_0\left(\frac{x_{\bar{l}}}{r_w}r\right)\bar{n}_0(r)}{\lambda_D^2\left[\left(\frac{x_{l'}}{r_w}\right)^2+k_m^2\right]\frac{r_w^2}{2}\mathrm{J}_1^2(x_{l'})}. \tag{203}$$

Comparing Eq. (184) to Eq. (203), we obtain the following relation between $\hat{\mathbf{e}}_0^\mu$ and $\mathbf{e}_0^\mu$:

$$(\hat{\mathbf{e}}_0^\mu)^{\bar{l}m}=\lambda_D^2\left[\left(\frac{x_{\bar{l}}}{r_w}\right)^2+k_m^2\right]\frac{r_w^2}{2}\mathrm{J}_1^2(\mathrm{x}_{\bar{l}})(\mathbf{e}_0^\mu)^{\bar{l}\mathrm{m}}. \tag{204}$$

2. First order in ε

Analysis of the first-order correction to the eigenmodes follows similar steps as for the 1D model of Sec. II, except that the matrix $\mathbf{M}_0^{mm}$ is not symmetric so both left and right eigenvectors must be used.

To the first order in ε, dispersion relation is given by

$$\mathbf{M}_0(\bar{\omega}_0^\mu).\mathbf{e}_1^\mu+\bar{\omega}_1^\mu\partial_{\bar{\omega}}\mathbf{M}_0(\bar{\omega}_0^\mu).\mathbf{e}_0^\mu+\mathbf{M}_1(\bar{\omega}_0^\mu).\mathbf{e}_0^\mu=0. \tag{205}$$

Taking the product of Eq. (205) from the left side with the left eigenvector $\hat{\mathbf{e}}_0^\mu$ and using Eq. (202), the first term will be eliminated. We can then solve for $\bar{\omega}_1^\mu$ and obtain

$$\bar{\omega}_1^\mu=-\frac{\hat{\mathbf{e}}_0^\mu.\mathbf{M}_1(\bar{\omega}_0^\mu).\mathbf{e}_0^\mu}{\hat{\mathbf{e}}_0^\mu.\partial_{\bar{\omega}}\mathbf{M}_0(\bar{\omega}_0^\mu).\mathbf{e}_0^\mu}=-\frac{(\hat{\mathbf{e}}_0^\mu)^m.\mathbf{M}_1^{mm}(\bar{\omega}_0^\mu).(\mathbf{e}_0^\mu)^m}{(\hat{\mathbf{e}}_0^\mu)^m.\partial_{\bar{\omega}}\mathbf{M}_0^{mm}(\bar{\omega}_0^\mu).(\mathbf{e}_0^\mu)^m}. \tag{206}$$

The real part of $\bar{\omega}_1^\mu$ gives a correction of order ε to the mode frequency and the imaginary part gives an order ε correction to the damping rate. The numerator of Eq. (206) can be evaluated using Eqs. (C1), (C5), and (184). We note that Eqs. (C1) and (C5) show that $\mathbf{M}_1^{mm}(\bar{\omega}_0^\mu)$ is a real function of $\mathrm{W}(\bar{\omega}_0^\mu/m)$ and $\bar{\omega}_0^\mu$; that is, $\mathbf{M}_1^{mm}$ is real if $\mathrm{W}(\bar{\omega}_0^\mu/m)$ and $\bar{\omega}_0^\mu$ are real. Furthermore, the denominator of Eq. (206) is also a real function of $\mathrm{W}(\bar{\omega}_0^\mu/m)$ and $\bar{\omega}_0^\mu$. This follows from Eq. (182) and identity (68). Therefore, the right hand side of Eq. (206) is a real function of $\mathrm{W}(\bar{\omega}_0^\mu/m)$ and $\bar{\omega}_0^\mu$, which we call $f(\mathrm{W},\bar{\omega}_0^\mu)$. Eq. (206) can therefore be written as

$$\bar{\omega}_1^\mu=f(\mathrm{W},\bar{\omega}_0^\mu). \tag{207}$$

We can then obtain the first-order correction to the damping rate by taking the imaginary part of this equation, substituting $\bar{\omega}_0^\mu=\bar{\omega}_{0r}^\mu+i\bar{\gamma}_0^\mu$ and Taylor expanding in $\bar{\gamma}_0^\mu$

$$\bar{\gamma}_1^\mu=\bar{\gamma}_0^\mu\partial_{\bar{\omega}}f(\mathrm{W},\bar{\omega}_0^\mu), \tag{208}$$

noting that $\mathrm{W}(\bar{\omega}_0^\mu/m)$ is real. This shows that $\bar{\gamma}_1^\mu$ is directly proportional to the zeroth order damping rate $\bar{\gamma}_0^\mu$. As a result, when $\bar{\omega}_0^\mu\gg m$, $\bar{\gamma}_1^\mu$ is also exponentially small.

Figure 11 shows the change in mode frequency versus the applied squeeze potential. As in the 1D case, the squeeze causes a decrease in the mode frequency, as the modes axial sloshing motion is impeded by the squeeze potential.

The first order correction to the eigenmode is obtained from Eq. (205) as

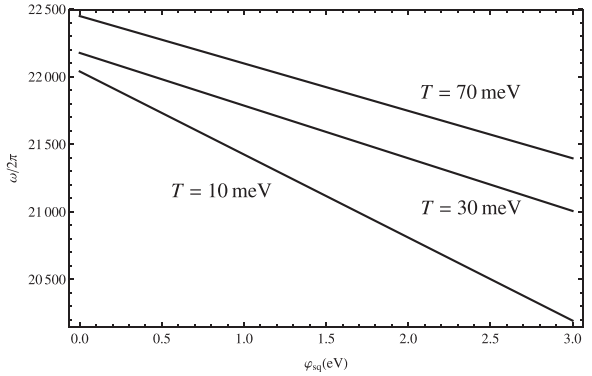

FIG. 11. Plot of the change in mode frequency for axial mode $m=1$ versus the applied squeeze potential, in a plasma of $L=10\,\text{cm}$, $\omega_p = 1.15\times10^6\,\text{rad/s}$, $r_p \approx 0.4\,\text{cm}$, and $r_w = 2.86\,\text{cm}$ for temperatures $T=10\,\text{meV}$, $T=30\,\text{meV}$, and $T=70\,\text{meV}$.

$$(\mathbf{e}_1^\mu)^j = -(\mathbf{M}_0^{jj}(\bar\omega_0^\mu))^{-1}.\mathbf{M}_1^{jm}(\bar\omega_0^\mu).(\mathbf{e}_0^\mu)^m, \quad j\neq m. \tag{209}$$

In the above equation, index j represents the axial Fourier mode number and radial indices are implicit. We also used the fact that the matrix $\mathbf{M}_0$ is block-diagonal in the axial modes (see Eq. (199)), which implies that its inverse is also block diagonal, with matrices $(\mathbf{M}_0^{jj})^{-1}$ in each block.

Equation (209) applies only for the components $(\mathbf{e}_l^\mu)^j$ with $j\neq m$. The $j=m$ term takes more work. For $j=m$, Eq. (205) becomes

$$\mathbf{M}_0^{mm}\cdot(\mathbf{e}_1^\mu)^m + [\bar\omega_1^\mu\partial_{\bar\omega}\mathbf{M}_0^{mm}(\bar\omega_0^\mu) + \mathbf{M}_1^{mm}(\bar\omega_0^\mu)]\cdot(\mathbf{e}_0^\mu)^m = 0. \tag{210}$$

To solve this equation, note that $\mathbf{M}_0^{mm}(\bar\omega_0^\mu)$ has a set of right and left eigenvectors $\mathbf{E}^n$ and $\hat{\mathbf{E}}^n$, respectively, with non-zero eigenvalues, in addition to the right and left eigenvector $(\mathbf{e}_0^\mu)^m$ and $(\hat{\mathbf{e}}_0^\mu)^m$ whose eigenvalue is zero (see Eqs. (200) and (202)). These other eigenvectors satisfy

$$\mathbf{M}_0^{mm}(\bar\omega_0^\mu)\cdot\mathbf{E}^n = \lambda_n\mathbf{E}^n \tag{211}$$

and[12]

$$\hat{\mathbf{E}}^n\cdot\mathbf{M}_0^{mm}(\bar\omega_0^\mu) = \lambda_n\hat{\mathbf{E}}^n. \tag{212}$$

We solve Eq. (210) by expanding $(\mathbf{e}_1^\mu)^m$ in the set of right eigenvectors (assuming they form a complete set)

$$(\mathbf{e}_1^\mu)^m = \sum_n c_n\mathbf{E}^n. \tag{213}$$

Note that we neglect the eigenvector with zero eigenvalue in this sum since, by assumption, $(\mathbf{e}_1^\mu)^m$ is orthogonal to this mode (which is included in the zeroth order). Substituting Eq. (213) into Eq. (210), and applying a left eigenvector yields the solution

$$c_n = -\frac{\hat{\mathbf{E}}^n\cdot[\bar\omega_1^\mu\partial_{\bar\omega}\mathbf{M}_0^{mm}(\bar\omega_0^\mu) + \mathbf{M}_1^{mm}(\bar\omega_0^\mu)]\cdot(\mathbf{e}_0^\mu)^m}{\lambda_n\hat{\mathbf{E}}^n\cdot\mathbf{E}^n}, \tag{214}$$

where we have used orthogonality of left and right eigenvectors, $\hat{\mathbf{E}}^{\bar n}\cdot\mathbf{E}^n = 0$ [provided $\lambda_{\bar n}\neq\lambda_n$].[12]

Note that the inversion of matrix $\mathbf{M}_0^{jj}$ in Eq. (209) can be carried out only when $\text{Det}[\mathbf{M}_0^{jj}]\neq 0$. This condition will not be satisfied in cases where degeneracies exist among the unsqueezed eigenmodes,[13] i.e., when $\bar\omega_0^\mu = \bar\omega_0^{\mu'}$ for unsqueezed modes μ and μ'. Fortunately, for the particular cases studied here, no such degeneracies appear. In Ref. 13, degeneracies occurred because ideal cold fluid theory was used; but here Landau-damping of high-order modes breaks the degeneracies.

Using Eq. (185), the squeezed eigenmode $\mu=(n_r,m)$ up to the first order in ε is

$$\begin{aligned}\delta\varphi^\mu(r,z,t) = {}& 2\delta\phi_0^\mu(r,z)e^{-\gamma t}\cos(\omega_r t)\\ &+2\,\text{Re}[\delta\phi_1^\mu(r,z)]e^{-\gamma t}\cos(\omega_r t)\\ &+2\,\text{Im}[\delta\phi_1^\mu(r,z)]e^{-\gamma t}\sin(\omega_r t),\end{aligned} \tag{215}$$

where

$$\delta\phi_1^\mu(r,z) = \varepsilon\sum_{l'\neq l}\sum_{m'\neq m}(\mathbf{e}_1^\mu)^{l'm'}\mathrm{J}_0\left(\frac{x_{l'}}{r_w}r\right)\cos[k_{m'}(z+L/2)]. \tag{216}$$

Since elements of $\mathbf{e}_0^\mu$ are linearly proportional to $|\delta\phi^\mu|$ and elements of $\mathbf{e}_1^\mu$ are linear combinations of elements of $\mathbf{e}_0^\mu$, both real and imaginary part of $\delta\phi_1^\mu(r,z)$ are linearly proportional to $|\delta\phi^\mu|$. Figures 12(a) and 12(b), respectively, depict the contour plots of the $\cos(\omega_r t)$ and $\sin(\omega_r t)$ time dependent part of the change to the $m=1$, $n_r=1$ eigenmode due to a squeeze potential, which are given, respectively, by the relations (215) and (216).

3. Second order in ε

Evidently, damping from the squeeze is second order in ε, just as in Sec. IV. The second order dispersion relation is given by Eq. (105)

$$\begin{aligned}&\mathbf{M}_0(\bar\omega_0^\mu).\mathbf{e}_2^\mu + \frac{(\bar\omega_0^\mu)^2}{2}\partial_{\bar\omega}^2\mathbf{M}_0(\bar\omega_0^\mu).\mathbf{e}_0^\mu + \bar\omega_2^\mu\partial_{\bar\omega}\mathbf{M}_0(\bar\omega_0^\mu).\mathbf{e}_0^\mu\\ &+\bar\omega_1^m\partial_{\bar\omega}\mathbf{M}_1(\bar\omega_0^\mu).\mathbf{e}_0^\mu + \mathbf{M}_1(\bar\omega_0^\mu).\mathbf{e}_1^\mu + \bar\omega_1^m\partial_{\bar\omega}\mathbf{M}_0(\bar\omega_0^\mu).\mathbf{e}_1^\mu\\ &+\mathbf{M}_2(\bar\omega_0^\mu).\mathbf{e}_0^\mu = 0.\end{aligned} \tag{217}$$

In order to solve for $\bar\gamma_2^\mu$ we take the imaginary part of the product of Eq. (217) with $\hat{\mathbf{e}}_0^\mu$. As for the derivations for the 1D case given by Eqs. (102) through (105), for $\bar\omega_0^\mu \gg m$, terms 1, 2, 4, and 6 are zero. As a result, the second order damping rate is given by

$$\bar\gamma_2^m = -\frac{\text{Im}\left[\sum_{j=1}^{\infty}(\hat{\mathbf{e}}_0^\mu)^m.\mathbf{M}_1^{mj}(\bar\omega_0^\mu).(\mathbf{e}_1^\mu)^j\right] + (\hat{\mathbf{e}}_0^\mu)^m.\text{Im}\mathbf{M}_2^{mm}(\bar\omega_0^\mu).(\mathbf{e}_0^\mu)^m}{(\hat{\mathbf{e}}_0^\mu)^m.\partial_{\bar\omega}\text{Re}\mathbf{M}_0^{mm}(\bar\omega_0^\mu).(\mathbf{e}_0^\mu)^m}, \tag{218}$$

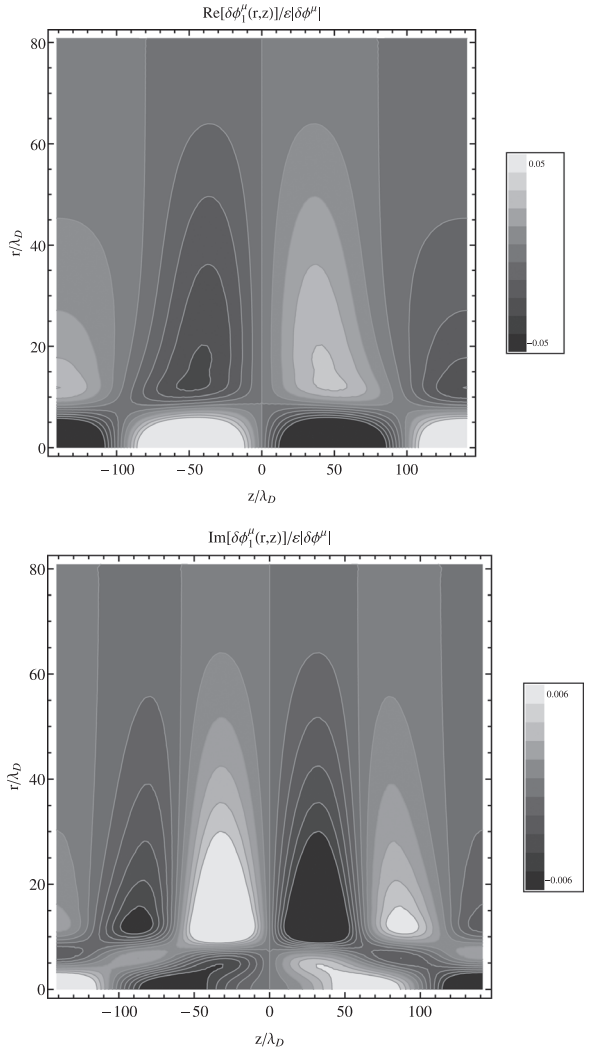

FIG. 12. Contour plots of the real and imaginary part of $\delta\phi_1^{\mu}(r,z)$, the change in the spatial dependence of the eigenmode due to squeeze potential, for the lowest-order mode $\mu=(1,1)$. $\mathrm{Re}[\delta\phi_1^{\mu}(r,z)]$ depicted in Fig. 12(a) has a $\cos(\omega_r t)$ time dependence and $\mathrm{Im}[\delta\phi_1^{\mu}(r,z)]$ depicted in Fig. 12(b) has a $\sin(\omega_r t)$ time dependence. The z axis extends from $-L/2$ to $L/2$ and the r axis extends from 0 to r_w. Plasma parameters are the same as for Fig. 7.

where $(\mathbf{e}_1^{\mu})^j$ is given by Eq. (209). Figure 13 shows the damping rate versus the applied squeezed potential for various temperatures using relations (201), (208), and (218), for typical confined plasma parameters. The second order damping rate is the result of resonant wave-particle interaction. Thus,

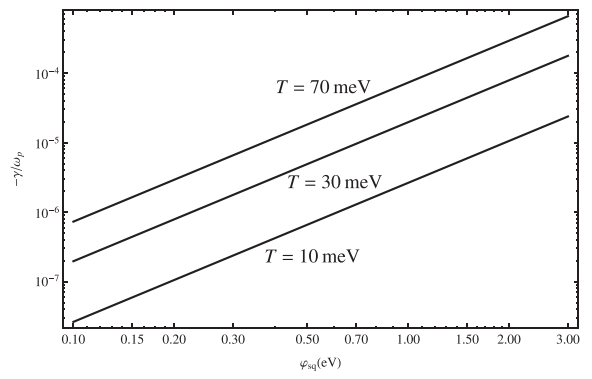

FIG. 13. Plot of the damping rate of axial mode $m=1$ versus the applied squeeze potential, in a plasma with same parameters as Fig. 11.

lowering the temperature will move the resonances in phase space to energies where the plasma is less populated, i.e., to higher phase velocities compared to the thermal velocity. As a result, lowering the temperature results in smaller damping rates.

V. CONCLUSION

In this paper, we have explored the effect of an applied squeeze potential on the frequency, damping and spatial form of TG modes. The presence of a squeeze potential results in additional resonant wave-particle interactions at the bounce frequencies $\omega_b = \omega/n$, which enhances the mode damping rate. There are two different reasons for these extra resonances to be generated: (i) The squeeze potential modifies the unperturbed orbits of the particles in such a way that a single cosine wave in position space is seen by the particles (as a function of time) as perturbed, containing higher harmonics with amplitudes of order φ_s/T. (ii) The shape of the mode potential in position space is also modified and contains higher harmonics of amplitudes $\mathcal{O}(\varphi_s/T)$. Our analysis shows that in the regime where $\varphi_s/T \ll 1$ and $\omega/k_m v_T \gg 1$, the mode damping rate has a quadratic dependence on the amplitude of the applied squeeze potential $|\varphi_{sq}|$, while, for low-order TG modes, the frequency shift due to squeeze is first-order in the squeeze potential. This behavior is consistent with experimental results. A detailed comparison to experiments will be presented in a separate paper.

In the theory presented here, we assume that the squeeze is applied slowly so that at every stage the plasma is in a thermal equilibrium state, described by a rigid-rotor Boltzmann distribution. However, in experiments, the squeeze may be applied rapidly, so that while the distribution remains Boltzmann along any given field line, the plasma is no-longer a rigid rotor. In the following work, we will generalize our results to account for effects such as this, where the squeezed plasma is not in a full thermal equilibrium state.

ACKNOWLEDGMENTS

This work was carried out under NSF Contract No. PHY0903877 and DOE Contract No. DE-SC0002451.

APPENDIX A: ORBIT CALCULATIONS

For a small squeeze potential such that $\varphi_s/T \ll 1$, the energy of a majority of particles is much larger than φ_s. We would like to expand the functions of energy in the system in terms of the smallness ordering parameter ε introduced in Eq. (23), assuming that adding the squeeze potential will result in a first order perturbative correction to these functions. Thus, for passing particles, which have scaled energies $u > \varepsilon\bar{\varphi}_s$, we expand the functions of energy in terms of ε to first order in ε. From Eq. (27), we calculate the period of the orbit for a passing particle at energy u which orbits the whole length of the plasma

$$\tau(u) = 2\int_{-\frac{L}{2}}^{\frac{L}{2}} \frac{dz}{v_T\sqrt{2(u-\varepsilon\bar{\varphi}_1(z))}}, \tag{A1}$$

$$\omega_b \approx \omega_0\left[1-\varepsilon\frac{\langle\bar{\varphi}_1(z)\rangle}{2u}\right], \tag{A2}$$

where the symbol $\langle\ldots\rangle$ represents the spatial average along the length of plasma L. Here, $\tau_0 = 2L/v_T\sqrt{2u}$ and $\omega_0 = \frac{\pi}{L}v_T\sqrt{2u}$ are, respectively, the time period and the bounce frequency of the motion of particle with energy u in the absence of the squeeze potential. The angle variable as a function of z, for $v>0$ is given by

$$\begin{aligned}\psi &= \frac{2\pi}{\tau}\int_{-L/2}^{z}\frac{dz'}{v(z')}\\ &\approx \frac{\pi}{L}\left[z+\frac{L}{2}+\varepsilon\int_{-L/2}^{z}dz'\frac{\{\bar{\varphi}_1(z')\}}{2u}\right].\end{aligned} \tag{A3}$$

In the above equation, we substituted $\tau(E)$ from Eq. (A1). Furthermore, we defined $\{\bar{\varphi}_1(z)\} = \bar{\varphi}_1(z) - \langle\bar{\varphi}_1(z)\rangle$, which is the size of the deviation of $\bar{\varphi}_1(z)$ from its spatial average $\langle\bar{\varphi}_1(z)\rangle$. For $v<0$, we have

$$\psi = \pi - \frac{\pi}{L}\left[z-L/2+\varepsilon\int_{-L/2}^{z}dz'\frac{\{\bar{\varphi}_1(z')\}}{2u}\right]. \tag{A4}$$

Thus, the angle variable can be written in terms of the angle variable in the absence of squeeze, plus a first order correction due to the squeeze potential

$$\psi = \psi_0 + \psi_1, \tag{A5}$$

$$\begin{aligned}\psi_0 &= \frac{\pi}{L}[z+L/2], \qquad v>0\\ &= \pi - \frac{\pi}{L}[z-L/2], \quad v<0,\end{aligned} \tag{A6}$$

$$\psi_1 = \varepsilon\,\mathrm{sign}(v)\frac{\pi}{L}\left[\int_{-L/2}^{z}dz'\frac{\{\bar{\varphi}_1(z')\}}{2u}\right]. \tag{A7}$$

The action variable is

$$\begin{aligned}I &= \frac{1}{2\pi}\oint p_z dz = \pi^{-1}\int_{-L/2}^{L/2} m_q v_T\sqrt{2u}(1-\varepsilon\bar{\varphi}_1(z)/u)^{1/2}dz\\ &\approx \frac{m_q v_T\sqrt{2u}L}{\pi}\left[1-\varepsilon\frac{\langle\bar{\varphi}_1\rangle}{2u}\right].\end{aligned} \tag{A8}$$

Comparing Eq. (A8) with Eq. (A2), we get the following relation:

$$I = m_q\omega_b\frac{L^2}{\pi^2}. \tag{A9}$$

Since in Eq. (A8), action variable I is given as a function of energy, we can reverse this relation to obtain energy as a function of I to the first order of perturbation

$$u = \frac{\pi^2 I^2}{2m_q L^2 T} + \varepsilon\langle\bar{\varphi}_1\rangle. \tag{A10}$$

The position dependent part of the mode potential $\delta\varphi(z)$ can be written as a(periodic) function of action-angle variable $\delta\varphi(z) = \delta\varphi(\psi, I)$. Furthermore, we can Fourier expand $\delta\varphi$ in terms of action-angle variables and calculate the nth Fourier component

$$\begin{aligned}\delta\varphi_n(I) &= \frac{1}{2\pi}\int_0^{2\pi}e^{-in\psi}\delta\varphi(z)d\psi\\ &\approx \delta\varphi_n^{(0)}(I) + \frac{1}{2\pi}\int_0^{2\pi}e^{-in(\psi_0+\psi_1)}\delta\varphi(z)(d\psi_0+d\psi_1)\\ &\approx \delta\varphi_n^{(0)}(I) + \frac{1}{2\pi}\int_0^{2\pi}(d\psi_1 - in\psi_1 d\psi_0)e^{-in\psi_0}\delta\varphi(z)\\ &\approx \delta\varphi_n^{(0)}(I) + \frac{1}{2\pi}\int_0^{2\pi}d\left(\psi_1 e^{-in\psi_0}\right)\delta\varphi(z).\end{aligned} \tag{A11}$$

Integrating by parts on the last line of Eq. (A11), since $\psi_1(z=\pm L/2)=0$, we obtain

$$\delta\varphi_n(I) \approx \delta\varphi_n^{(0)}(I) - \frac{1}{2\pi}\int_0^{2\pi}\psi_1 e^{-in\psi_0}d(\delta\varphi(z)), \tag{A12}$$

where $\delta\varphi_n^{(0)}(I)$ is the Fourier component in terms of action-angle variables, in the absence of squeeze potential for which ψ_0 is given by Eq. (A5)

$$\begin{aligned}\delta\varphi_n^{(0)}(I) &= \frac{1}{2\pi}\int_0^{2\pi}e^{-in\psi_0}\delta\varphi(z)d\psi_0\\ &= \int_{-L/2}^{L/2}\frac{dz}{L}\cos\left[\frac{n\pi}{L}\left(z+\frac{L}{2}\right)\right]\delta\varphi(z).\end{aligned} \tag{A13}$$

Using Eqs. (A6) and (A7), we can write Eq. (A11) as

$$\begin{aligned}&\delta\varphi_n(I) - \delta\varphi_n^{(0)}(I)\\ &\quad= -\varepsilon\int_{-L/2}^{L/2}\frac{dz}{L}\cos\left[\frac{n\pi}{L}\left(z+\frac{L}{2}\right)\right]\int_{-\frac{L}{2}}^{z}dz'\frac{\{\bar{\varphi}_1(z')\}}{2u}\frac{d}{dz}\delta\varphi(z).\end{aligned} \tag{A14}$$

We will now use these results to determine the Fourier coefficients $C_m^n(I)$ given by Eq. (34), to the first order in ε. For the squeeze potential, we use the symmetric form given by Eq. (17). From the wave potential $\delta\varphi(z,t)$ given by Eq. (31), we can see that the wave is a superposition of cosine waves. For the mth cosine, we substitute $\cos[\frac{m\pi}{L}(z+\frac{L}{2})]$ for $\delta\varphi(z)$. Substituting from Eq. (31) in Eq. (A13), we obtain the unsqueezed Fourier components

$$\begin{aligned}[C_m^n(I)]^{(0)} &= \int_{-L/2}^{L/2}\frac{dz}{L}\cos\left[\frac{n\pi}{L}(z+L/2)\right]\delta\bar{\phi}\cos\left[\frac{m\pi}{L}(z+L/2)\right]\\ &= \frac{1}{2}(\delta_{n,m}+\delta_{n,-m}).\end{aligned} \tag{A15}$$

Using the relation

$$\int_{-L/2}^{z}\frac{\{\bar{\varphi}_1(z')\}}{2u}dz' = \sum_{\bar{m}=1}^{\infty}\frac{\bar{\varphi}^1_{\bar{m}}}{2u}\frac{L}{2\pi\bar{m}}\sin\left[2\pi\frac{\bar{m}}{L}(z+L/2)\right],$$

first we calculate the perturbation to the mth Fourier mode in angle space

$$\begin{aligned}
&C^m_m(I) - [C^m_m(I)]^{(0)}\\
&= \varepsilon\int_{-L/2}^{L/2}\frac{dz}{L}\frac{m\pi}{L}\cos\left[\frac{m\pi}{L}(z+L/2)\right]\sin\left[\frac{m\pi}{L}(z+L/2)\right]\\
&\quad\times\sum_{m'=1}^{\infty}\frac{\bar{\varphi}^1_{m'}}{2u}\frac{L}{2\pi m'}\sin\left[2\pi\frac{m'}{L}(z+L/2)\right]\\
&= \varepsilon\int_0^L\frac{dy}{L}\frac{m\pi}{2L}\sin\left[\frac{2m\pi}{L}y\right]\sum_{m=1}^{\infty}\frac{\bar{\varphi}^1_m}{2u}\frac{L}{2\pi m'}\sin\left[2\pi m'\frac{y}{L}\right]\\
&= \frac{\bar{\varphi}^1_m}{16}\left(\frac{\varepsilon}{u}\right). \qquad \text{(A16)}
\end{aligned}$$

Now we calculate the perturbation to the nth Fourier mode, where $n \neq \pm m$

$$\begin{aligned}
C^n_m(I) &= \varepsilon\int_0^L\frac{dy}{L}\frac{m\pi}{L}\cos\left(\frac{n\pi y}{L}\right)\sin\left(\frac{n\pi y}{L}\right)\sum_{m'=1}^{\infty}\frac{\bar{\varphi}^1_{m'}}{2u}\\
&\quad\times\frac{L}{2\pi m'}\sin\left[2\pi m'\frac{y}{L}\right]\\
&= \varepsilon m\int_0^L\frac{\pi dy}{L}\frac{1}{2}\left(\sin\left[(n+m)\frac{\pi y}{L}\right]\right.\\
&\quad\left.+\sin\left[(m-n)\frac{\pi y}{L}\right]\right)\sum_{m'=1}^{\infty}\frac{\bar{\varphi}^1_{m'}}{4\pi m' u}\sin\left[2\pi m'\frac{y}{L}\right]\\
&= \varepsilon\sum_{m'=1}^{\infty}m\int_0^L\frac{\pi dy}{L}\frac{1}{4}\left(\cos\left[(n+m-2m')\frac{\pi y}{L}\right]\right.\\
&\quad-\cos\left[(n+m+2m')\frac{\pi y}{L}\right]+\cos\left[(m-n-2m')\frac{\pi y}{L}\right]\\
&\quad\left.-\cos\left[(m-n+2m')\frac{\pi y}{L}\right]\right)\frac{\varphi^1_{m'}}{4\pi m' u}. \qquad \text{(A17)}
\end{aligned}$$

Finally, the above integral simplifies to

$$\begin{aligned}
C^n_m(I) = \varepsilon\sum_{m'=1}^{\infty}&(\delta_{n,-m+2m'} - \delta_{n,-m-2m'} + \delta_{n,m-2m'}\\
&- \delta_{n,m+2m'})\frac{m\bar{\varphi}^1_{m'}}{4\pi m' u}. \qquad \text{(A18)}
\end{aligned}$$

In the above Kronecker delta functions, if m is odd, n must be odd and if m is even, n must be even in order to get a non-zero result. Since $m' > 0$, we can further simplify Eq. (A18) to obtain

$$C^n_m(I) = \frac{m}{8}\left(\frac{\bar{\varphi}^1_{|m-n|/2}}{m-n} + \frac{\bar{\varphi}^1_{|m+n|/2}}{m+n}\right)\left(\frac{\varepsilon}{u}\right), \quad n \neq \pm m. \qquad \text{(A19)}$$

For both n and m odd or both even. In summary, we have

$$C^n_m(I) = [C^m_m(I)]^{(0)} + \alpha^n_m\varepsilon/u, \qquad \text{(A20)}$$

$$[C^m_m(I)]^{(0)} = \frac{1}{2}\delta_{|n|,m}, \qquad \text{(A21)}$$

$$\begin{aligned}
\alpha^n_m &= \frac{m}{8}\left[\frac{\bar{\varphi}^1_{|m-n|/2}}{m-n} + \frac{\bar{\varphi}^1_{|m+n|/2}}{m+n}\right], \quad n \neq m\\
&= \frac{\bar{\varphi}^1_m}{16}, \quad n = \pm m. \qquad \text{(A22)}
\end{aligned}$$

For the rz system, the Fourier series expansion for the scaled Debye shielded squeeze potential $\bar{\varphi}_1(r,z)$, defined in Eq. (155), is given by

$$\bar{\varphi}_1(r,z) = \langle\bar{\varphi}_1(r,z)\rangle_z + \sum_{m=1}^{\infty}\bar{\varphi}^1_m(r)\cos\left[2\pi\frac{m}{L}(z+L/2)\right].$$

We can perform similar calculations, starting from Eqs. (158) through (162). Fourier coefficients of the squeezed rz system to the first order in ε are given by

$$C^n_m\left(r,\frac{\varepsilon}{u}\right) = \frac{1}{2}\delta_{|n|,m} + \alpha^n_m(r)\frac{\varepsilon}{u}, \qquad \text{(A23)}$$

where coefficients $\alpha^n_m(r)$ are functions of radius given by

$$\begin{aligned}
\alpha^n_m(r) &= \frac{m}{8}\left[\frac{\bar{\varphi}^1_{|m-n|/2}(r)}{m-n} + \frac{\bar{\varphi}^1_{|m+n|/2}(r)}{m+n}\right], \quad n \neq m\\
&= \frac{\bar{\varphi}^1_m(r)}{16}, \quad n = \pm m. \qquad \text{(A24)}
\end{aligned}$$

APPENDIX B: MATRIX CALCULATION

In order to obtain expressions for the zeroth, first, and second order dispersion matrices $\mathbf{M}_0$, $\mathbf{M}_1$, and $\mathbf{M}_2$ from Eq. (50), we need the functional form of $u_n(\varepsilon)$ for $\varepsilon \ll 1$, where $u_n(\varepsilon)$ is the scaled energy at which $\omega_b(u_n) = \omega/n$. In dimensionless form, this relation is

$$\bar{\omega}_b(u_n,\varepsilon) = \bar{\omega}/n. \qquad \text{(B1)}$$

We first expand $\bar{\omega}_b(u,\varepsilon)$ to second order in ε, obtaining, from Eq. (A1)

$$\bar{\omega}_b = 1/\int_{-L/2}^{L/2}dz/L\frac{1}{\sqrt{2u}}\left(1+\frac{\varepsilon\bar{\varphi}_1(z)}{u}+\frac{3}{8}\varepsilon^2\frac{\bar{\varphi}^2_1(z)}{u^2}\right), \qquad \text{(B2)}$$

which implies

$$\bar{\omega}_b(u,\varepsilon) = \sqrt{2u}\left[1-\frac{\varepsilon}{2u}\langle\bar{\varphi}_1\rangle+\frac{\varepsilon^2}{4u^2}\left(\langle\bar{\varphi}_1\rangle^2-\frac{3}{2}\langle\bar{\varphi}^2_1\rangle\right)+\ldots\right]. \qquad \text{(B3)}$$

We can then invert this expression to solve Eq. (B1) for u_n, writing $u_n = u_{n0} + \varepsilon u_{n1} + \ldots$ and collecting terms of the same order in ε. The result is

$$u_n = \frac{\bar{\omega}^2}{2n^2} + \langle\bar{\varphi}_1\rangle\varepsilon + \frac{3}{2}\left(\frac{n}{\bar{\omega}}\right)^2(\langle\bar{\varphi}^2_1\rangle - \langle\bar{\varphi}_1\rangle^2)\varepsilon^2 + \ldots. \qquad \text{(B4)}$$

As a result, we have to second order in ε

$$e^{-u_n} = e^{-\frac{\bar{\omega}^2}{2n^2}}\left(1 - \langle\bar{\varphi}_1\rangle\varepsilon - \frac{3}{2}\left(\frac{n}{\bar{\omega}}\right)^2(\langle\bar{\varphi}_1^2\rangle - \langle\bar{\varphi}_1\rangle^2)\varepsilon^2 + \frac{1}{2}\langle\bar{\varphi}_1\rangle^2\varepsilon^2 + \ldots\right). \tag{B5}$$

Furthermore, we expand $1/\langle e^{-\varepsilon\bar{\varphi}_1}\rangle$

$$\begin{aligned} 1/\langle e^{-\varepsilon\bar{\varphi}_1}\rangle &= 1/\left(1 - \langle\bar{\varphi}_1\rangle\varepsilon + \frac{1}{2}\langle\bar{\varphi}_1^2\rangle\varepsilon^2 + \ldots\right) \\ &= 1 + \langle\bar{\varphi}_1\rangle\varepsilon - \frac{1}{2}\langle\bar{\varphi}_1^2\rangle\varepsilon^2 + \langle\bar{\varphi}_1\rangle^2\varepsilon^2\ldots. \end{aligned} \tag{B6}$$

Thus, we have

$$\frac{e^{-u_n}}{\langle e^{-\varepsilon\bar{\varphi}_1}\rangle} = e^{-\frac{\bar{\omega}^2}{2n^2}}\left(1 - \left(\frac{3}{2}\left(\frac{n}{\bar{\omega}}\right)^2 + \frac{1}{2}\right)\left[\langle\bar{\varphi}_1^2\rangle - \langle\bar{\varphi}_1\rangle^2\right]\varepsilon^2 + \ldots\right). \tag{B7}$$

We also need $d\bar{\omega}_b(u_n,\varepsilon)/du$. Taking the derivative of Eq. (B3) and using Eq. (B4) implies

$$\frac{d\bar{\omega}_b(u_n,\varepsilon)}{du} = \frac{n}{\bar{\omega}}\left(1 + 3\left(\frac{n}{\bar{\omega}}\right)^4(\langle\bar{\varphi}_1^2\rangle - \langle\bar{\varphi}_1\rangle^2)\varepsilon^2 + \ldots\right). \tag{B8}$$

We now use these results to expand the dispersion matrix $\mathbf{M}(\bar{\omega},\varepsilon)$ in powers of ε. To zeroth order, we use the lowest order forms in Eq. (44), $\bar{\omega}_b = \sqrt{2u}$ (from Eq. (B3)), and $C_{m,n} = \delta_{m,|n|}/2$ from Eq. (A21). This implies

$$M_0^{mn}(\bar{\omega}) = \delta_{mn}\left[1 + \frac{1}{K_m^2\lambda_D^2}\mathrm{W}(\bar{\omega}/m)\right]. \tag{B9}$$

The first order correction is found using the first-order expansions of $1/\langle e^{-\varepsilon\bar{\varphi}_1}\rangle$, $\bar{\omega}_b$ and $C_{m,n}$ in Eq. (44). This results in the expression

$$\begin{aligned} M_1^{mp}(\bar{\omega}) = &-\frac{8(K_m\lambda_D)^{-2}}{\sqrt{2\pi}}\sum_{n=1}^{\infty}\Bigg\{-\bar{\varphi}_s\frac{\bar{\omega}_b(0,0)}{(\bar{\omega}/n)^2 - \bar{\omega}_b(0,0)^2}C_p^n(0)C_m^n(0) \\ &+\left[\langle\bar{\varphi}_1\rangle\int_0^{\infty}du\frac{\bar{\omega}_b(u,0)e^{-u}}{(\bar{\omega}/n)^2 - \bar{\omega}_b(u,0)^2} + \int_0^{\infty}du\partial_\varepsilon\bar{\omega}_b(u,0)\frac{(\bar{\omega}/n)^2 + \bar{\omega}_b(u,0)^2}{((\bar{\omega}/n)^2 - \bar{\omega}_b(u,0)^2)^2}e^{-u}\right]C_p^n(0)C_m^n(0) \\ &+\int_0^{\infty}du\frac{\bar{\omega}_b(u,0)e^{-u}}{(\bar{\omega}/n)^2 - \bar{\omega}_b(u,0)^2}\left(\partial_\varepsilon C_p^n(0)C_m^n(0) + \partial_\varepsilon C_m^n(0)C_p^n(0)\right)\Bigg\}. \end{aligned} \tag{B10}$$

The first term on the right hand side arises from expansion in ε of the lower bound in the u-integral in Eq. (42). This is zero since from Eq. (B3) we have $\bar{\omega}_b(0,0) = 0$. The second term arises from expansion of $1/\langle\mathbf{e}^{-\varepsilon\bar{\varphi}_1}\rangle$ using Eq. (B6), and the last two terms arise from expansion of $\bar{\omega}_b$ and C_m^n, respectively. From Eq. (B3), we have

$$\bar{\omega}_b(u,0) = \sqrt{2u}, \quad \partial_\varepsilon\bar{\omega}_b(u,0) = -\langle\bar{\varphi}_1\rangle/\sqrt{2u}. \tag{B11}$$

Using Eqs. (B11) and (A20), the remaining terms on the right hand side of Eq. (B10) can be simplified to obtain

$$\begin{aligned} M_1^{mp}(\bar{\omega}) = &-\frac{2(K_m\lambda_D)^{-2}}{\sqrt{2\pi}}\Bigg\{\langle\bar{\varphi}_1\rangle\int_0^{\infty}du\frac{\sqrt{2u}e^{-u}}{(\bar{\omega}/m)^2 - 2u}\delta_{mp} - \langle\bar{\varphi}_1\rangle\int_0^{\infty}du\frac{(\bar{\omega}/m)^2 + 2u}{\sqrt{2u}((\bar{\omega}/m)^2 - 2u)^2}e^{-u}\delta_{mp} \\ &+2\int_0^{\infty}du\frac{\sqrt{2u}e^{-u}}{u((\bar{\omega}/m)^2 - 2u)}\alpha_p^m + 2\int_0^{\infty}du\frac{\sqrt{2u}e^{-u}}{u((\bar{\omega}/p)^2 - 2u)}\alpha_m^p\Bigg\}. \end{aligned} \tag{B12}$$

Now, using integration by parts we can show that

$$\langle\bar{\varphi}_1\rangle\int_0^\infty du\frac{(\bar{\omega}/m)^2+2u}{\sqrt{2u}((\bar{\omega}/m)^2-2u)^2}e^{-u}=\langle\bar{\varphi}_1\rangle\int_0^\infty due^{-u}\frac{d}{du}\left(\frac{\sqrt{2u}}{(\bar{\omega}/m)^2-2u}\right)=\langle\bar{\varphi}_1\rangle\int_0^\infty du\frac{\sqrt{2u}}{(\bar{\omega}/m)^2-2u}e^{-u}. \tag{B13}$$

Thus, the first two terms in Eq. (B12) cancel and we are left with

$$M_1^{mp}(\bar{\omega})=-\frac{2(K_m\lambda_D)^{-2}}{\sqrt{2\pi}}\left\{2\int_0^\infty du\frac{\sqrt{2u}e^{-u}}{u((\bar{\omega}/m)^2-2u)}\alpha_p^m+2\int_0^\infty du\frac{\sqrt{2u}e^{-u}}{u((\bar{\omega}/p)^2-2u)}\alpha_m^p\right\}. \tag{B14}$$

Using the following relation, we further simplify $M_1^{mp}(\bar{\omega})$

$$\begin{aligned}\int_0^\infty du\frac{\sqrt{2u}e^{-u}}{u((\bar{\omega}/m)^2-2u)}&=\int_0^\infty du\frac{2\sqrt{2u}}{(\bar{\omega}/m)^2}\left(\frac{1}{2u}+\frac{1}{(\bar{\omega}/m)^2-2u}\right)e^{-u}\\&=\frac{\sqrt{2}}{(\bar{\omega}/m)^2}\mathrm{P}\int_0^\infty\frac{e^{-u}}{\sqrt{u}}du+\frac{2}{(\bar{\omega}/m)^2}\mathrm{P}\int_0^\infty\frac{\sqrt{2u}}{(a/m)^2-2u}\mathrm{e}^{-u}du\\&=\frac{m^2}{\bar{\omega}^2}\sqrt{2\pi}[1-\mathrm{W}(\bar{\omega}/m)]\,,\end{aligned} \tag{B15}$$

where $\mathrm{W}(x)$ is defined in Eq. (55). As a result, we obtain

$$M_1^{mp}(\bar{\omega})=-\frac{4}{K_m^2\lambda_D^2}\left(\frac{m^2}{\bar{\omega}^2}[1-\mathrm{W}(\bar{\omega}/m)]\alpha_p^m+\frac{p^2}{\bar{\omega}^2}[1-\mathrm{W}(\bar{\omega}/p)]\alpha_m^p\right). \tag{B16}$$

For $\mathbf{M}_2$, we note that we only need $\mathrm{Im}\mathbf{M}_2$ in our lowest-order expression for the damping rate due to squeeze. Applying Eqs. (B4), (B5), (B7), and (B8) to Eq. (44), we obtain the following pure series form for $\mathrm{Im}\,\mathbf{M}(\bar{\omega},\varepsilon)$:

$$\begin{aligned}\mathrm{Im}M^{mp}(\bar{\omega},\varepsilon)=&\frac{4\pi}{\lambda_D^2K_m^2\sqrt{2\pi}}\sum_{n=1}^\infty\frac{\bar{\omega}}{n}e^{-\bar{\omega}^2/2n^2}\left(1-\left(\frac{3}{2}\left(\frac{n}{\bar{\omega}}\right)^2+\frac{1}{2}\right)\left[\langle\bar{\varphi}_1^2\rangle-\langle\bar{\varphi}_1\rangle^2\right]\varepsilon^2+\ldots\right)\\&\times\left(1-3\left(\frac{n}{\bar{\omega}}\right)^4[\langle\bar{\varphi}_1^2\rangle-\langle\bar{\varphi}_1\rangle^2]\varepsilon^2+\ldots\right)\left(\delta_{nm}/2+\frac{2n^2}{\bar{\omega}^2}\alpha_m^n\varepsilon+(\beta_m^n-\langle\bar{\varphi}_1\rangle\alpha_m^n)\left(\frac{2n^2}{\bar{\omega}^2}\right)^2\varepsilon^2+\ldots\right)\\&\times\left(\delta_{np}/2+\frac{2n^2}{\bar{\omega}^2}\alpha_p^n\varepsilon+(\beta_p^n-\langle\bar{\varphi}_1\rangle\alpha_p^n)\left(\frac{2n^2}{\bar{\omega}^2}\right)^2\varepsilon^2+\ldots\right),\end{aligned} \tag{B17}$$

where we also used the following series expansion, which is obtained in detail in Appendix A to the first order(second order coefficients β_m^n are not evaluated since they do not contribute to our results)

$$\begin{aligned}C_m^n(\varepsilon/u_n)&=\delta_{nm}/2+(\varepsilon/u_n)\alpha_m^n+(\varepsilon/u_n)^2\beta_m^n+\ldots\\&=\delta_{nm}/2+\varepsilon\frac{2n^2}{\bar{\omega}^2}\alpha_m^n+\varepsilon^2(\beta_m^n-\langle\bar{\varphi}_1\rangle\alpha_m^n)\left(\frac{2n^2}{\bar{\omega}^2}\right)^2+\ldots.\end{aligned} \tag{B18}$$

The zeroth, first, and second order $\mathrm{Im}\mathbf{M}$ are found by collecting terms in Eq. (B17)

$$\mathrm{Im}\,M_0^{mp}(\bar{\omega})=\frac{4\pi}{\lambda_D^2K_m^2\sqrt{2\pi}}\frac{\bar{\omega}}{m}e^{-\bar{\omega}^2/2m^2}\delta_{m,p}/4, \tag{B19}$$

$$\mathrm{Im}\,M_1^{mp}(\bar{\omega})=\frac{4\pi}{\lambda_D^2K_m^2\sqrt{2\pi}}\left[e^{-\bar{\omega}^2/2p^2}\frac{p}{\bar{\omega}}\alpha_m^p+e^{-\bar{\omega}^2/2m^2}\frac{m}{\bar{\omega}}\alpha_p^m\right], \tag{B20}$$

$$\begin{aligned}\mathrm{Im}\,M_2^{mp}(\bar{\omega})=&\frac{4\pi}{\lambda_D^2K_m^2\sqrt{2\pi}}\left[-\frac{\bar{\omega}}{m}e^{-\bar{\omega}^2/2m^2}\left(3\left(\frac{m}{\bar{\omega}}\right)^4+\frac{3}{2}\left(\frac{m}{\bar{\omega}}\right)^2+\frac{1}{2}\right)\left[\langle\bar{\varphi}_1^2\rangle-\langle\bar{\varphi}_1\rangle^2\right]\delta_{m,p}/4+2e^{-\bar{\omega}^2/2p^2}(\beta_m^p-\langle\bar{\varphi}_1\rangle\alpha_m^p)\left(\frac{p}{\bar{\omega}}\right)^3\right.\\&\left.+2e^{-\bar{\omega}^2/2m^2}(\beta_p^m-\langle\bar{\varphi}_1\rangle\alpha_p^m)\left(\frac{m}{\bar{\omega}}\right)^3+\sum_{n=1}^\infty4\left(\frac{n}{\bar{\omega}}\right)^3e^{-\bar{\omega}^2/2n^2}\alpha_m^n\alpha_p^n\right].\end{aligned} \tag{B21}$$

Note that the expression for $\mathrm{Im}\,\mathbf{M}_1$ agrees with the imaginary part of Eq. (B16).

APPENDIX C: MATRIX CALCULATION FOR THE RZ SYSTEM

In order to carry out a perturbation expansion of the dispersion relation of the rz system given by Eq. (177), in terms of ε as the smallness parameter, we need the series expansion of $M^{\bar{l}l\bar{m}m}$ given by Eq. (179) in terms of ε. We write this matrix as

$$M^{\bar{l}l\bar{m}m} = \delta_{\bar{l}l}\delta_{\bar{m}m} + \frac{\int_0^{r_w} r dr \mathrm{J}_0\left(\frac{x_l}{r_w}r\right)\mathrm{J}_0\left(\frac{x_{\bar{l}}}{r_w}r\right)\bar{n}_0(r)b(r,\varepsilon)\mathcal{M}^{\bar{m}m}(r,\bar{\omega},\varepsilon)}{\left[\left(\frac{x_{\bar{l}}}{r_w}\right)^2 + k_{\bar{m}}^2\right]\frac{r_w^2}{2}\mathrm{J}_1^2(x_{\bar{l}})}, \tag{C1}$$

where

$$b(r,\varepsilon) = \frac{\left\langle \mathbf{e}^{-\varepsilon\varphi_1(r,z)/T}\right\rangle_z}{\langle \bar{n}_0(r)e^{-\varepsilon\varphi_1(r,z)/T}/\langle\bar{n}_0(r)\rangle_r\rangle_{rz}} \tag{C2}$$

is a Boltzmann prefactor due to variation of the squeeze potential with radius, and

$$\mathcal{M}^{\bar{m}m}(r,\bar{\omega},\varepsilon) = -\frac{8}{\sqrt{2\pi}\,\lambda_D^2\langle e^{-\epsilon\bar{\varphi}_1(r,z)}\rangle_z}\sum_{n=1}^{\infty}\int_{\varepsilon\bar{\varphi}_1(r,0)}^{\infty} du\,\frac{\bar{\omega}_b e^{-u}}{(\bar{\omega}/n)^2-\bar{\omega}_b^2}C_m^n\left(r,\frac{\varepsilon}{u}\right)C_{\bar{m}}^n\left(r,\frac{\varepsilon}{u}\right) \tag{C3}$$

is the same matrix as appeared in the 1D calculation (the second term in Eq. (44)) (aside from multiplicative constant K_m^{-2} that does not appear in Eq. (C3)). We expanded this matrix in ε in Appendix B and can use those results to obtain the required ε expansion here. The zeroth order matrix is (see Eq. (B9))

$$\mathcal{M}_0^{\bar{m}m} = \delta_{\bar{m}m}\mathrm{W}(\bar{\omega}/m)/\lambda_D^2, \tag{C4}$$

and the first-order correction $\mathcal{M}_1^{\bar{m}m}$ is given by Eq. (B16) (multiplied by K_m^2)

$$\mathcal{M}_1^{\bar{m}m} = -\frac{4}{\lambda_D^2}\left\{\frac{\bar{m}^2}{\bar{\omega}^2}[1-\mathrm{W}(\bar{\omega}/\bar{m})]\alpha_{\bar{m}}^m + \frac{m^2}{\bar{\omega}^2}[1-\mathrm{W}(\bar{\omega}/m)]\alpha_m^{\bar{m}}\right\}. \tag{C5}$$

Let us call the second-order correction $\mathcal{M}_2^{\bar{m}m}$; the imaginary part of this matrix was evaluated in Eq. (B21). Now, expanding $b(r,\varepsilon)$ to second-order yields $b(r,\varepsilon) = 1 + \varepsilon b_1(r) + \varepsilon^2 b_2(r)$ where

$$b_1(r) = \frac{\varepsilon}{T}\left(\langle\bar{n}_0(r)\varphi_1\rangle_{rz}/\langle\bar{n}_0(r)\rangle_r - \langle\varphi_1\rangle_z\right) \tag{C6}$$

and

$$b_2(r) = \frac{1}{T^2}\left(\frac{1}{2}\langle\varphi_1^2\rangle_z + \left(\langle\bar{n}_0\varphi_1/\langle\bar{n}_0\rangle_z\rangle_{rz}\right)^2 - \frac{1}{2}\langle\bar{n}_0\varphi_1^2/\langle\bar{n}_0\rangle_r\rangle_{rz} - \langle\varphi_1\rangle_z\langle\bar{n}_0\varphi_1/\langle\bar{n}_0\varphi_1/\langle\bar{n}_0\rangle_r\rangle_{rz}\right), \tag{C7}$$

and thus the combination $b(r,\varepsilon)\mathcal{M}^{\bar{m}m}(r,\bar{\omega},\varepsilon)$ has the following expansion, up to second order:

$$\begin{aligned} b(r,\varepsilon)\mathcal{M}^{\bar{m}m}(r,\bar{\omega},\varepsilon) = {} & \mathcal{M}_0^{\bar{m}m}(r,\bar{\omega}) + \varepsilon\left(\mathcal{M}_1^{\bar{m}m}(r,\bar{\omega}) + \mathcal{M}_0^{\bar{m}m}(r,\bar{\omega})b_1(r)\right) \\ & + \varepsilon^2\left(\mathcal{M}_2^{\bar{m}m}(r,\bar{\omega}) + \mathcal{M}_1^{\bar{m}m}(r,\bar{\omega})b_1(r) + \mathcal{M}_0^{\bar{m}m}(r,\bar{\omega})b_2(r)\right). \end{aligned} \tag{C8}$$

Using Eqs. (C1), (C4), and (C8), we obtain the following explicit form for the zeroth order matrix $M_0^{\bar{l}l\bar{m}m}$:

$$M_0^{\bar{l}l\bar{m}m} = \delta_{\bar{m}m}\left(\delta_{\bar{l}l} + 2\mathrm{W}(\bar{\omega}/m)\frac{\int_0^{r_w} r\,dr\bar{n}_0(r)\mathrm{J}_0(x_{\bar{l}}r/r_w)\mathrm{J}_0(x_l r/r_w)}{\lambda_D^2\left[x_{\bar{l}}^2 + k_{\bar{m}}^2 r_w^2\right]\mathrm{J}_1^2(x_{\bar{l}})}\right), \tag{C9}$$

and using Eq. (C5), we obtain the first order matrix $M_1^{\bar{l}l\bar{m}m}$

$$M_1^{\bar{l}l\bar{m}m} = \frac{\int_0^{r_w} r\,dr\bar{n}_0(r)\mathrm{J}_0(x_{\bar{l}}r/r_w)\mathrm{J}_0(x_l r/r_w)\left[\mathcal{M}_1^{\bar{m}m}(r,\bar{\omega}) + \mathcal{M}_0^{\bar{m}m}(r,\bar{\omega})b_1(r)\right]}{\lambda_D^2\left[x_{\bar{l}}^2 + k_{\bar{m}}^2 r_w^2\right]\mathrm{J}_1^2(x_{\bar{l}})}. \tag{C10}$$

For the second order matrix, we only require the imaginary part, given by

$$\mathrm{Im}\, M_2^{\bar{l}\,l\,\bar{m}m} = -\frac{\int_0^{r_w} r\, dr \bar{n}_0(r) \mathrm{J}_0(x_{\bar{l}} r/r_w) \mathrm{J}_0(x_l r/r_w) \left[\mathrm{Im}\, \mathcal{M}_2^{\bar{m}m}(r,\bar{\omega}) + \mathrm{Im}\, \mathcal{M}_1^{\bar{m}m}(r,\bar{\omega}) b_1(r) + \mathrm{Im}\, \mathcal{M}_0^{\bar{m}m}(r,\bar{\omega}) b_2(r)\right]}{\lambda_D^2 \left[x_{\bar{l}}^2 + k_{\bar{m}}^2 r_w^2\right] \mathrm{J}_1^2(x_{\bar{l}})}, \tag{C11}$$

where $\mathrm{Im}\, \mathcal{M}_2^{\bar{m}m}(r,\bar{\omega})$ is given by Eq. (B21) (except for the factor of K_m^{-2}).

[1]A. W. Trivelpiece and R. W. Gould, J. Appl. Phys. **30**, 1784 (1959).
[2]T. J. Hilsabeck and T. M. O'Neil, Phys. Plasmas **10**, 3492 (2003).
[3]D. H. E. Dubin and Y. A. Tsidulko, Phys. Plasmas **18**, 062114 (2011).
[4]C. F. Driscoll, A. A. Kabantsev, and D. H. E. Dubin, "Transport, damping and wave-couplings from chaotic and collisional neoclassical transport," AIP Conf. Proc. **1521**, 15 (2013).
[5]S. A. Prasad and T. M. O'Neil, Phys. Fluids **26**, 665 (1983).
[6]N. A. Krall and A. W. Trivelpiece, *Principles of Plasma Physics* (San Francisco Press, San Francisco, 1986), Chap. 8, pp. 375–383.
[7]D. H. E. Dubin, Phys. Plasmas **12**, 042107 (2005).
[8]J. P. Boyd, J. Comput. Phys. **110**, 360 (1994).
[9]W. E. Schieser, *The Numerical Method of Lines* (Academic Press, 1991).
[10]D. H. E. Dubin, *Numerical and Analytical Methods for Scientists and Engineers Using Mathematica* (Wiley-Interscience, Hoboken, New Jersey, 2003), Chap. 2, p. 151.
[11]D. H. E. Dubin and T. M. O'Neil, Rev. Mod. Phys. **71**, 87 (1999).
[12]W. H. Press, B. P. Flannery, S. A. Teukolsky, and W. T. Vetterling, *Numerical Recipes: The Art of Scientific Computing*, 3rd ed. (Cambridge University Press, Cambridge, England, 2007), Chap. 11, p. 564.
[13]M. W. Anderson, T. M. O'Neil, D. H. E. Dubin, and R. W. Gould, Phys. Plasmas **18**, 102113 (2011).